Geological Quarterly, 2023, 67: 23
DOI: http://dx.doi.org/10.7306/gq.1693

Biostratigraphy, microfacies and reservoir quality of the Oligocene Qom Formation (Kharzan section, north-west of Ardestan, central Iran)

Asma AFTABI ARANI[1], Ali Reza ASHOURI[1], Jahanbakhsh DANESHIAN[2], Abbas GHADERI[1, *] and David A. WOOD[3]

[1] Ferdowsi University of Mashhad, Department of Geology, Faculty of Science, Mashhad, Iran; ORCID: 0009-0005-6345-7686 [A.A.A.], 0000-0002-2913-4913 [A.R.A.], 0000-0001-9404-7827 [A.G.]

[2] Kharazmi University of Tehran, Department of Geology, Faculty of Science, Tehran, Iran;ORCID: 0000-0001-5503-1216

[3] DWA Energy Limited, Lincoln, UK; ORCID: 0000-0003-3202-4069

Aftabi Arani, A., Ashouri, A.R., Daneshian, J., Ghaderi, A., Wood, D.A., 2023. Biostratigraphy, microfacies and reservoir quality of the Oligocene Qom Formation (Kharzan section, north-west of Ardestan, central Iran). Geological Quarterly, 67: 23, doi: 10.7306/gq.1693

Associate Editor: Michał Zatoń

The central Iran Basin is a region with unique environmental characteristics in which the Late Paleogene–Early Neogene benthic foraminifera display distinctive distributions and abundances that can assist in identifying the intervals with the best reservoir potential. Lipidocyclinid and miogypsinid zonal marker taxa in this region can be correlated with those in the SBZ23 region (European Basin), indicating an Oligocene (Chattian) age. With sedimentation of continental strata of the Upper Red Formation following the marine succession of the Qom Formation, it seems that the last Tethyan marine transgression in the Ardestan region in central Iran occurred in the Oligocene, and the Tethyan seaway was permanently closed during the Miocene. Seven carbonate microfacies and marl or silty marl facies were identified in the study area based on field investigations, textural analysis and faunal assemblages. These microfacies were deposited on an open-shelf carbonate platform in lagoonal, patch-reef, and open-marine belts that effectively define both inner and middle-shelf environments. Micritization, cementation, mechanical and chemical compaction, dissolution and fracturing are the most important diagenetic processes controlling reservoir quality in the Qom Formation. The investigation of these processes in the facies of the Qom formation in the Kharzan section revealed that intervals associated with shallow lagoonal depositional environments display better reservoir quality than other formation intervals, due to dissolution and fracturing.

Key words: Oligocene, benthic foraminifera, sedimentary environment, reservoir quality, Qom Formation, central Iran.

INTRODUCTION

The Qom Formation is one of central Iran's most important lithostratigraphic units because of its commercial productivity as a gas and oil reservoir. It requires detailed study due to its variable lithostratigraphic, biostratigraphic, and microfacies characteristics, as well as its extensive development in the Sanandaj-Sirjan, Urumieh–Dokhtar Magmatic Arc, and central Iran zones (Fig. 1A). The Qom Formation contains substantial hydrocarbon resources, making it the primary oil and gas exploration target in central Iran. Furthermore, the Qom Formation represents a crucial connective link between the eastern Tethys (the proto-Indian Ocean) and the western Tethys (the proto-Mediterranean Sea) regions.

The Oligocene–Miocene Qom Formation includes marl, limestone, gypsum and siliciclastic rocks.

Most micropalaeontological studies on this formation are based on planktonic and benthic foraminifera. In the past twenty years, many such studies have focused on the Qom Formation; some of the most relevant of these studies are shown in Table 1.

Most of these micropalaeontological studies have considered the Miocene (Aquitanian–Burdigalian) deposits of the Qom Formation in detail; however, a detailed analysis of the Oligocene deposits of this formation has been lacking.

This study evaluates a new stratigraphic section in central Iran focusing on Oligocene foraminifera. It has three main objectives: (1) detailing the biostratigraphy of the Qom Formation based on the distribution of large benthic foraminifera (LBF); (2) establishing the depositional settings of the Qom Formation in the Kharzan section using microfacies analysis; and, (3) investigating the diagenetic processes affecting the Qom Formation in the Kharzan Mountain region and its effect on reservoir qual-

* Corresponding author: e-mail: aghaderi@um.ac.ir

Received: November 14, 2022; accepted: May 17, 2023; first published online: September 19, 2023

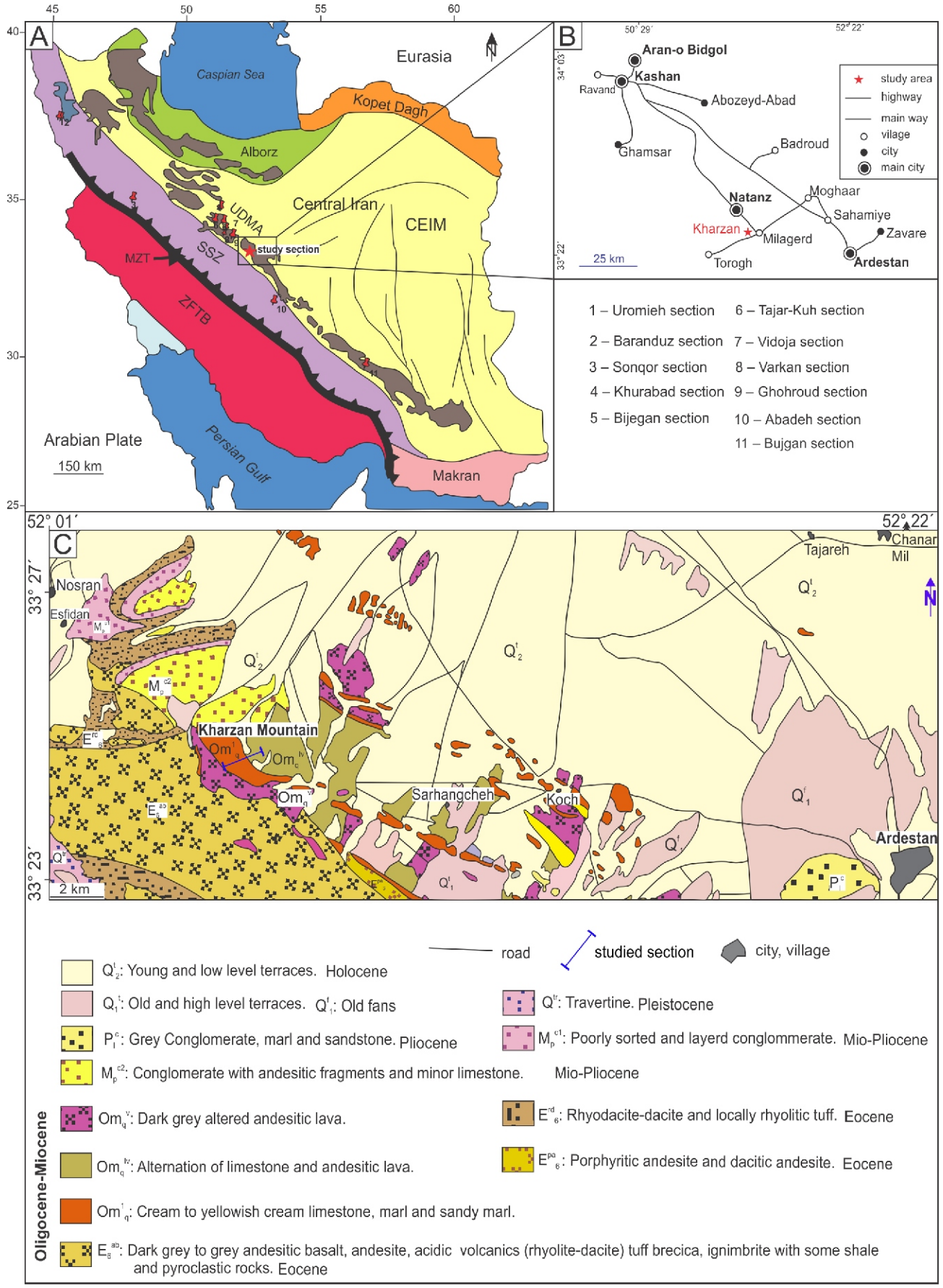

Fig. 1A – simplified geological map of Iran showing the main tectonic subdivisions and the location of the study section (modified after Agard et al., 2011); CEIM – Central East Iran Microplate, MZT – Main Zagros Thrust, SSZ – Sanandaj-Sirjan Zone, UDMA – Uromia Dokhtar Magmatic Arc, ZFTB – Zagros-Fold-Thrust Belt; geographical location of the section studied and adjacent sections; B – geographic map locating the section studied (modified after Iran view, 2020); C – geological map of the Kharzan area (modified after Radfar and Amini, 1999)

Table 1

Some of the most important studies done on the Qom Formation in Iran and their results

Author	Section	Location	Age	Fossils used for biostratigraphy	Geographical coordinates
Seyrafian and Torabi (2005)	–	Southern of Central Iran (North of Nain)	late Oligocene (Chattian)–early Miocene? (Aquitanian?)	Benthic Foraminifera	33° 04' 21" N 53° l0' 20" E
Daneshian and Dana (2007)	Deh Namak	Central Iran (East of Garmsar)	Early Miocene (Aquitanian to Early Burdigalian)	Benthic Foraminifera	35° 18' 21" to 35° 30'31" N 52° 43'17" to 52° 43'23" E
Khaksar and Moghaddam (2007)	–	Central Iran (South of Tehran)	Oligocene	Echinoderms	–
Hadavi et al. (2010)	Kamar-Kuh	North Central Iran	Miocene (Burdigalian–Serravalian)	Nannofossils	–
Behforouzi and Safari (2011)	Chenar area	Central Iran (northwestern Kashan)	Oligocene	Large Benthic Foraminifera	34° 05' N 51° 09' E
Seddighi et al. (2012)	–	Central Iran (27 km to Qom City)	Oligocene-Miocene (Chattian–Aquitanian)	Large Benthic Foraminifera	34?25′51.1″ N 51°07′114.8″ E
Amirshahkarami and Karavan (2015)	Kahak	Urumieh-Dokhtar magmatic arc	Oligocene (Rupelian–Chattian)–Miocene (Aquitanian–Burdigalian)	Benthic Foraminifera	–
Nouradini et al. (2015)	Bagh	Central Iran (Northeastern Isfahan)	early Miocene (Aquitanian)	Planktonic Foraminifera and Benthic Foraminifera	32?57′61″ N 52?01′95″ E
Daneshian and Ghanbari (2017)	Sad-e-Mosh-ampa, Sheikh Jaber	Northwest of Central Iran (Zanjan area)	Miocene (Burdigalian–Langhian)	Planktonic Foraminifera	–
Mohammadi et al. (2019)	Barzok	Central Iran (Southwester Kashan)	Oligocene (Rupelian)	Benthic Foraminifera	33°51'31'' N 51°9'14'' E
Daneshian and Dana (2019)	11 stratigraphic sections	North and Northwest Central Iran	Miocene (Aquitanian-Burdigalian)	Benthic Foraminifera	1 – Atari: 35?43′31″ N, 53°38′03″ E 2 – Aftar: 35?17′42″ N, 53°43′00″ E 3 – Deh Namak: 35?21′18″ N, 52°17′35.21″ E 4 – Ghasr-e-Bahram: 34°45′02″ N, 52°06′08″ E 5 – Southeast Niasar: 33?56′00″ N, 51°11′00″ E 6 – Sorkh Deh: 34?28′07″ N, 50°15′57″ E 7 – Barieh: 35?23′01″ N, 49°50′02″ E 8 – Meserghan: 35?19′03″ N, 49°45′40″ E 9 – Ghareh Gurghan: 35?49′00″ N, 49°19′00″ E 10 – Naghash: 35?39′42″ N, 49°16′50″ E 11 – Kohlou: 35?00′00″ N, 48°46′04″ E
Parandavar and Hadavi (2019)	Shurab (south of Qom) Navab Anticline (Southeast of Kashan)	Central Iran (Southeast the of Kashan, South of the Garmsar)	Oligocene-Miocene	Nannofossils	1 – Shurab: 34°25'N, 51°08'E 2 – Navab: 33°51'N, 51°38'E
Mohammadi (2022)	10 outcrop sections (Gonarestan, Tavakolabad, Bozdan, Bujan, Abadeh, Ghohroud, Varkan, Jazeh, Vidoja, Khurabad)	–	Oligocene–early Miocene (Rupelian–early Burdigalian)	Large Benthic Foraminifera	–

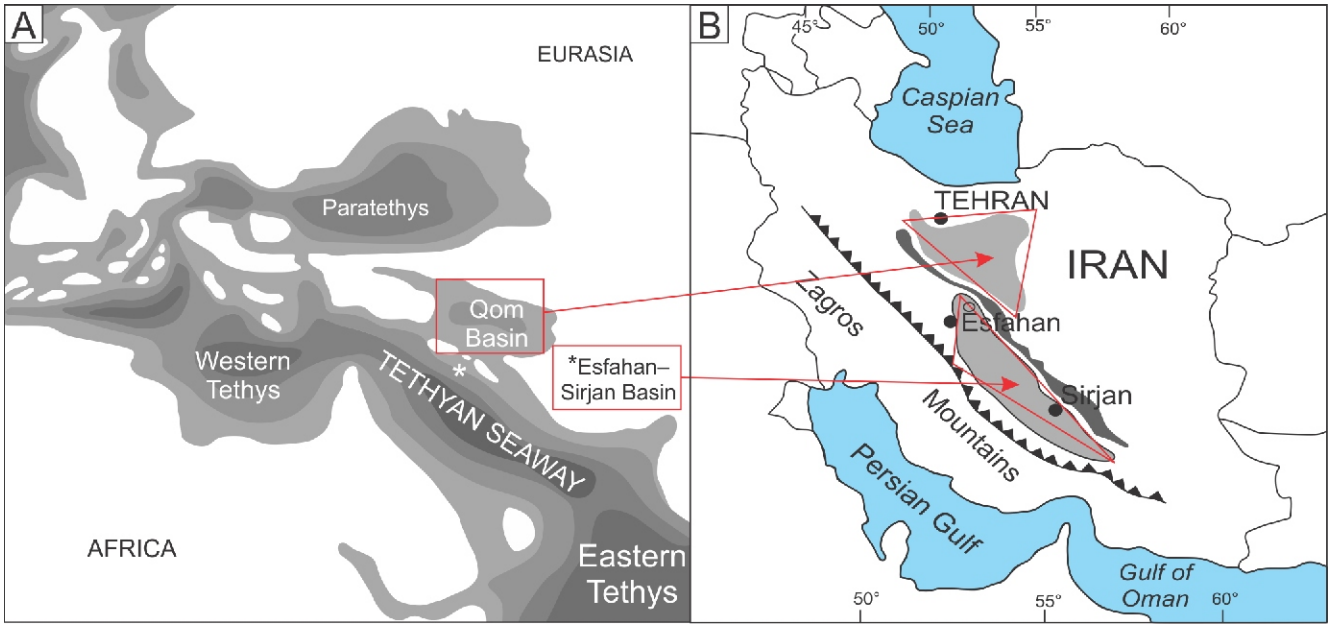

Fig. 2. The Tethyan Seaway and adjacent regions in the late Oligocene (modified from Harzhauser and Piller, 2007)

ity. This work combines biostratigraphy, lithofacies and diagenesis to assist in identifying the most prospective reservoir sequences in the Qom Formation of the Kharzan section.

GEOLOGICAL SETTING

The Qom basin is located within the Iranian plate on the southeastern margin of the Paratethys Sea. Its position and lithology are highly significant for understanding the palaeogeography, and reconstructing the distribution, of the Paratethys Sea from the Mediterranean Sea to the Indo-Pacific region during the late Oligocene to early Miocene interval (Stocklin and Setudehina, 1991; Khaksar and Moghaddam, 2007; Daneshian and Dana, 2007; Reuter et al., 2009; Mohammadi et al., 2011; Yazdi-Moghadam et al., 2011). The early Paleogene Tethys Ocean was broad and served as an extensive connection between large oceans to the east (Pacific) and west (Atlantic). The collision of the Atlantic and Pacific plates and subsequent subduction between the African and Arabian plates occurred during the late Eocene to early Oligocene epochs (Schuster and Wielandt, 1999). These events led to the disappearance of the Tethys Ocean via a transitional state as a narrow seaway. Not only did these events isolate much of the Northern Atlantic Ocean from the Pacific Ocean, but they also ultimately played a role in the formation of the Indian Ocean and the Mediterranean Sea. The palaeogeography of central Iran underwent substantial change as a consequence of these events. Initially, a volcanic island arc developed separating a fore-arc region from a back-arc depositional area during the Eocene. This was followed by the marine deposition of the Qom Formation from the Oligocene and throughout the early Miocene. The formation exhibits distinctive depositional environments related to the Esfahan–Sirjan fore-arc region and the Qom back-arc region (Schuster and Wielandt, 1999; Fig. 2).

MATERIAL AND METHODS

The stratigraphic section studied is located in the north-west of Ardestan (south-east of Natanz, East of Milajerd village, Kharzan Mountain) in central Iran (Fig. 1A). The coordinates of the section base are 33°24’36"N and 52°05’57"E, and the top are 33?24´50.9˝ N and 52?06´48.3˝E. Access to the study area is possible from the Qom–Kashan highway and Kashan–Ardestan main road to Kharzan Mountain. The Qom Formation succession in this area comprises 422 metres of limestone, argillaceous limestone, marl, and silty marl. These strata are overlain partly by the Lower Red Formation and partly by the Upper Red Formation with a disconformity (Figs. 1B, C and 3).

A total of 261 rock samples, taken every 1 to 2 metres, were systematically collected from the Qom Formation succession in the Kharzan section for detailed biostratigraphic and facies analysis.

One thin section from each lithified rock sample was prepared and studied under the polarizing microscope to identify the benthic foraminifera assemblage present and also to analyze the sedimentary facies and diagenetic processes affecting each sample.

Facies descriptions were determined based on field investigations and the microscopic analysis of the thin sections. The classification schemes of Dunham (1962) and Embry and Klovan (1971) were applied to describe the carbonate rocks. Depositional texture, grain size, the composition of grains and fossil content were all taken into account for microfacies interpretation. The Qom Formation facies at the Kharzan location studied were classified based on Flügel’s (2010) standard facies types. All the samples and thin sections evaluated are deposited in the Exploration Directorate National Iranian Oil Company (NIOCEXP) collection in Tehran, Iran.

Fig. 3A – contact between the Lower Red and Qom formations at outcrop; B – disconformity between the Qom and Upper Red formations in the Kharzan outcrop section (looking towards the south)

REGIONAL KNOWLEDGE AND CONTEXT OF OLIGO-MIOCENE BIOZONES

The previously established biozones for the Oligo-Miocene age range in Iran, especially those relating to the late Oligocene–early Miocene, are classified into three main groups:

1. Based on one or two stratigraphic sections (e.g., Nayebi, 1995);
2. Proposed based on a large number of stratigraphic sections (e.g., Wynd, 1965; Adams and Bourgeois, 1967; Rahaghi, 1980; Deighton, 1985; Baghbani et al., 1996; Laursen et al., 2009; Mohammadi, 2022);
3. Based on planktonic foraminifera (e.g., Daneshian et al., 2017; Daneshian and Ghanbari, 2017).

Among the studies mentioned, the biozonation proposed by Wynd (1965), Adams and Bourgeois (1967) and Laursen et al. (2009) relates to the Zagros Mountains region. On the other hand, the biozones proposed by Baghbani et al. (1996) and Mohammadi (2022) relate to the central Iran region, and the Deighton (1985) biozonation relates to the Makran zone. To date, no formal biozonation has been proposed for the Qom Formation in central Iran. Central Iran and the Zagros basin were geographically close during the Oligocene–Miocene (Bozorgnia, 1966), with connection initiated in the early Miocene (Aquitanian period; Adams and Bourgeois, 1967). Moreover, geochronological and faunal similarities exist between the

Asmari and Qom formations. These two factors make it realistic to apply the biozonations proposed for the Zagros Basin by Wynd (1965) and Adams and Bourgeois (1967) to the Qom Formation.

Nummulites and lepidocyclinid index species are common in the Oligocene Qom Formation and its equivalent in the Zagros Basin, the Asmari Formation, and have been used for biozonation (Mohammadi and Ameri, 2015). In a few sections, *Nummulites* species have been found alone in Rupelian, or lower Rupelian, strata whereas lepidocyclinids alone have been found in Chattian strata or Aquitanian formations (e.g., Bozorgnia and Kalantari, 1965; Kalantari, 1976; Amirshahkarami et al., 2007; Ehrenberg et al., 2007; Laursen et al., 2009; Amirshahkarami et al., 2010; Van Buchem et al., 2010; Yazdi-Moghadam, 2011; Mohammadi et al., 2013, 2015; Karavan et al., 2014; Mohammadi and Ameri, 2015; Taheri et al., 2017; Yazdi-Moghadam et al., 2018; Basso et al., 2019; Akbar-Baskalayeh et al., 2020; Allahkarampour Dill et al., 2018; Mohammadi, 2022). In Iran, Biozone No.57, the *Nummulites intermedius-Nummulites vascus* assemblage zone, was first proposed as an index for the Oligocene by Wynd (1965), who described the properties and biostratigraphic features of Oligocene–Miocene strata in the Asmari Formation in the south-west of Iran. Specifically, Wynd (1965) introduced 7 assemblage biozones: numbers 56, 57, 58, 59, 60, 61 and 62. These are: 56 – the *Lepidocyclina–Operculina–Ditrupa* assemblage zone; age: Oligocene–Miocene; 57 – the *Nummulites intermedius–Nummulites vascus* assemblage zone; age: Oligocene; 58 – the *Archaias operculiniformis* zone; age: Oligocene; 59 – the *Austrotrillina howchini–Peneroplis evolutus* assemblage zone; age: Miocene; 60 – the *Austrotrillina howchini–Peneroplis evolutus* assemblage zone; age: Miocene; and 61, 62 – the *Borelis melo curdica* assemblage zone; age: Miocene.

The *Nummulites–Eulepidina–Nephrolepidina* Assemblage Zone was also attributed to the Oligocene by Adams and Bourgeois (1967). These classical studies, although conducted on the Asmari Formation in the Zagros Mountains, are considered valid for the biozonation of the Qom Formation in central Iran. However, the Oligocene stages (Rupelian and Chattian) were not distinguished in either of those studies.

Previously in Iraq, larger benthic foraminifera (LBFs) have been used to establish the biozonation of the nine formations that make up the Kirkuk group by Bellen et al. (1959). In that study, the *Nummulites* group alone was attributed to the early Rupelian, the concomitant presence of *Nummulites* together with *Lepidocyclina* or *Lepidocyclina* alone was attributed to the middle Rupelian, and *Lepidocyclina* with *Miogypsinoides* or *Miogypsinoides* alone was attributed to the late Rupelian. Moreover, Sartorio and Venturini (1988) considered the last occurrence of *Nummulites* to mark the early Oligocene and the occurrence of *Meandropsina, Archaias, Austrotrillina, Lepidocyclina* and *Miogypsinoides* as the marker assemblage for the late Oligocene.

Shallow-water deposits of the Upper Paleocene–Lower Miocene in the North of Oman were studied by Racey (1994), who assigned the occurrence of *Nummulites* with *Eulepidina* and *Nephrolepidina* to the Chattian Stage, while *Nummulites* without these two genera to represent the Rupelian Stage. Also, Jones et al. (1994) assigned the occurrence of *Nummulites* without *Eulepidina* to the Rupelian and *Nummulites* together with *Eulepidina* to the late Rupelian–early Chattian.

Serra-Kiel et al. (1998) established twenty-six shallow benthic foraminiferal biozones (SBZs) in the Cenozoic Tethyan shallow basin based on different groups of LBFs. Twenty lower biozones (covering the Cretaceous/Paleogene and Eocene/Oligocene boundaries) and six upper biozones (Oligocene to Miocene/Pliocene boundary) were characterized by Cahuzac and Poignant (1997). Their biozonation was based on the benthic faunal succession of the southern European shallow basins, especially those of the Aquitaine region in France. They used the co-existence of both *Nummulites fichteli* and *Nummulites vascus* to represent the early Rupelian (= SB21), and *Eulepidina formosoides* alone to represent the late Rupelian (= SB22A). Also, they suggested that the presence of *Nummulites vascus* and *Nummulites fichteli* together with *Eulepidina* represented the early Chattian (= SB22B), and the coexistence of *Eulepidina* and *Miogypsinoides* represented the late Chattian (= SB23).

Based on strontium isotope data from three subsurface sections (Bibi Hakimeh, Marun, and Ahvaz) and one section at outcrop (Khaviz) in south-west Iran, Ehrenberg et al. (2007) considered the last occurrence of the *Nummulites* to have occurred one million years earlier than the Rupelian/Chattian boundary. They also identified *Spiroclypeous blanckenhorni* in the Chattian interval in Marun, Ahvaz and Khaviz sections, a result that agrees with the findings of Cahuzac and Poignant (1997). Ehrenberg et al. (2007), confirmed the Chattian age for *Archaias* proposed by Adams et al. (1983) across the Middle East. Additionally, Adams et al. (1983) considered the first occurrence of *Miogypsina* as an early Miocene index, whereas Ehrenberg et al. (2007) assigned this genus to the uppermost parts of the Chattian. Moreover, they considered *Borelis melo curdica* as a valid index taxon for the Burdigalian Stage.

Van Buchem et al. (2010), using biostratigraphic analysis and strontium isotope studies on the Oligocene–Miocene successions (Pabdeh and Asmari formations) of southwestern Iran, characterized three assemblage zones in the shallow deposits of the Asmari Formation. In ascending order, they are Assemblage A (with a high abundance of *Nummulites* indicative of the lowermost parts of the Oligocene), Assemblage B (with dominant occurrences of *Nummulites* and *Eulepidina* indicative of the Rupelian), and Assemblage C (with the dominant occurrence of *Eulepidina* without the *Nummulites* indicative of the Chattian).

RESULTS

The Qom Formation, which has a thickness of 422 metres, is situated above the Lower Red Formation. After analyzing 261 sedimentary rock samples collected from the Kharzan section, 49 genera and 59 species of benthic foraminifera were identified in this study. Geographical proximity existed between central Iran and the Zagros basin during the Oligocene-Miocene and the Asmari and Qom formations are of similar age and share faunal similarities. These two factors make it realistic to apply the biozonations proposed for the Zagros Basin by Wynd (1965) and Adams and Bourgeois (1967) to the Qom Formation. Wynd (1965) established an early framework for biostratigraphic criteria relating to the Asmari Formation. Subsequently, Adams and Bourgeois (1967) reviewed and improved this framework, but the Rupelian and Chattian remained undifferentiated. The larger benthic foraminiferal fauna recog-

nized in this section allowed the authors to compare the assemblage studied with coeval assemblages in the Middle East and Europe. Therefore, comparisons of the benthic foraminifera in the Kharzan section with biozonations such as those of Bellen et al. (1959), Sartorio and Venturini (1988), Racey (1994), Jones et al. (1994), Serra-Kiel et al. (1998), Cahuzac and Poignant (1997), Ehrenberg et al. (2007) and Van Buchem et al. (2010), suggest that the age of the Qom Formation in the studied area is Chattian. Also, according to the distribution chart, most of the larger foraminiferal taxa assemblages from the Kharzan section, coupled with the presence of *Miogypsinoides* spp., and the association with lepidocyclinids, correspond to assemblages already described from Europe. Therefore, the European standard shallow benthic zonation can be extended to the Kharzan section in Iran, indicating that the Qom Formation shows a good correlation with SBZ23, which determines its age to be late Oligocene (Chattian). Based on fossil assemblages, lithology, sedimentary characteristics and the textures of the outcrop samples from the Kharzan section, seven different carbonate microfacies types have been recognized throughout the Qom Formation. These are silty mudstone, imperforate foraminiferal wackestone-packstone, imperforate foraminiferal packstone-grainstone, red algal-foraminiferal packstone-grainstone, coral boundstone, coralline red algal-coral packstone-rudstone, perforate foraminiferal wackestone-packstone, and marl or silty marl facies. In the section analyzed, the texture, fossil assemblage and relative stratigraphic positions of the microfacies of the Qom Formation show the characters of an open shelf carbonate platform, subdivided into lagoonal, patch-reef, and open-marine belts. A marginal-reef environment was not observed. Based on the distribution of the foraminifera and vertical facies relationships, two major depositional environments were identified in the late Oligocene succession in the study section. These are inner shelf and middle open shelf environments. The facies association in the middle shelf strata mainly comprises flat, thin-walled, large tests of lepidocyclinid and nummulitid, and medium to small robust, ovate hyaline, foraminifera and fragmented bioclasts. Towards the proximal mid-shelf, the presence of robust, ovate, and lens-shaped, perforate foraminifera increases. The abundance of larger foraminifera such as *Neorotalia* and *Amphistegina* together with corallinaceans indicate a shallow, open-marine environment near and below the fair-wave base on the proximal mid-shelf (Geel, 2000; Pomar, 2001a, b; Brandano and Corda, 2002; Cosovic et al., 2004). The association is dominated by robust and ovate tests of perforate foraminifera, which reflect shallower water conditions than those containing larger and flat perforate foraminifera (Beavington-Penney and Racey, 2004; Barattolo et al., 2007). This diverse faunal assemblage suggests that deposition took place in a marine environment of normal salinity. The inner shelf mainly consists of *Neorotalia* and corallinacean debris, mainly in the form of perforate and imperforate foraminifera and bioclasts. Hyaline perforated foraminifera belong to small robust and ovate tests of rotalids and amphisteginids, whereas the imperforate foraminifera with porcellaneous walls are mainly represented by miliolids, *Peneroplis* and *Borelis*. The contemporaneous existence of normal marine perforate foraminifera and platform interior imperforate foraminifera reflect the absence of an effective barrier between the inner and mid-shelf (Geel, 2000; Romero et al., 2002). The co-occurrence of these groups indicates that deposition took place in an open marine lagoon (Nebelsick et al., 2001; Rasser and Nebelsick, 2003). The main constituents of the proximal inner shelf are imperforate foraminifera, which tend to be associated with very shallow, often restricted marine carbonate facies (Bassi et al., 2007). The abundance of foraminifera with non-perforate walls and the complete absence of normal marine biota indicates that deposition took place in a restricted shelf lagoon (Hallock and Glenn, 1986; Geel, 2000; Romero et al., 2002). The lime mud of Mf2 is interpreted as the shallowest part of the inner shelf environment deposited in protected conditions (Murray, 2006). The Qom Formation is the main objective of oil and gas exploration in central Iran. For this reason, it is very important to investigate the properties of the reservoir and the processes that cause its quality to change. The study of the carbonate strata of the Qom Formation has revealed that diagenetic processes in part degraded (due to cementation and compaction), and in part improved (due to dissolution and fracturing) its reservoir quality. Evidence of diagenesis is widespread throughout the formation in the study area. In general, zones associated with shallow lagoonal facies display better reservoir quality than other facies due to the greater influence and preservation of dissolution zones and fractures.

DISCUSSION

FORAMINIFERA ASSEMBLAGES PRESENT IN THE KHARZAN SECTION

Analysis of the Qom Formation's benthic foraminiferal content led to the identification of 49 genera and 59 species in the Kharzan section studied. These are listed in Appendix 1. Planktonic foraminifera are absent from the section studied. Consequently, age dating and biostratigraphic correlations were established based on the LBF assemblages observed.

To date, no occurrence of Miogypsinidae taxa has been reported from the Rupelian and older strata of Iran. *Miogypsinoides* spp. was found 82 metres above the base of the Kharzan section. There it coexists with the observed occurrence of an assemblage of foraminifera consisting of *Amphistegina* spp., *Asterigerina rotula, Austrotrillina asmariensis, A. paucialveolata, A. striata, Borelis haueri, B. merici, B. pygmaea, Brizalina* spp., *Bullalveolina* spp., *Carpenteria* spp., *Dendritina rangi, Eulepidina* sp., *E. dilatata, Haddonia* spp., *Halkyardia maxima, H.* spp., *Heterostegina* spp., *Idalina* spp., *Lenticulina* spp., *Massilina* spp., *Miogypsinoides* spp., *Neorotalia vienotti, Nephrolepidina* spp., *Operculina complanata, Peneroplis evolutus, P. thomasi, Praerhapydionina* sp., *Pseudolituonella reichelli, Risananeiza pustulosa, Schlumbergerina* spp., *Spirolina* sp., *Sphaerogypsina globulus, Triloculina tricarinata, T. trigonula* and *Valvulina* sp.1. That assemblage suggests a Chattian age for that zone in the Kharzan section. That age is consistent with the findings of Van Buchem et al. (2010), who considered the predominance of lepidocyclinids without *Nummulites* to represent the Chattian. It is also compatible with the biozonation of Cahuzac and Poignant (1997), which assigned the simultaneous presence of *Eulepidina* and *Miogypsinoides* to the late Chattian. The age range spanning the Qom Formation in the Kharzan section is therefore equivalent to biozone SB23 of Cahuzac and Poignant (1997).

Appendix 1 provides a comparison of the foraminiferal assemblage observed in the Kharzan section combined with the adjacent Iranian sections of Oligocene age. Some of the genera and species reported from the Kharzan section are unique to that section and identified for the first time by this study. The taxa *Risananeiza pustulosa* and *Borelis merici* have been reported for the first time from the deposits of the Qom Formation in the Kharzan section. Also, *Miogypsinoides* spp., the zone marker of the Chattian age range, is observed only in this section.

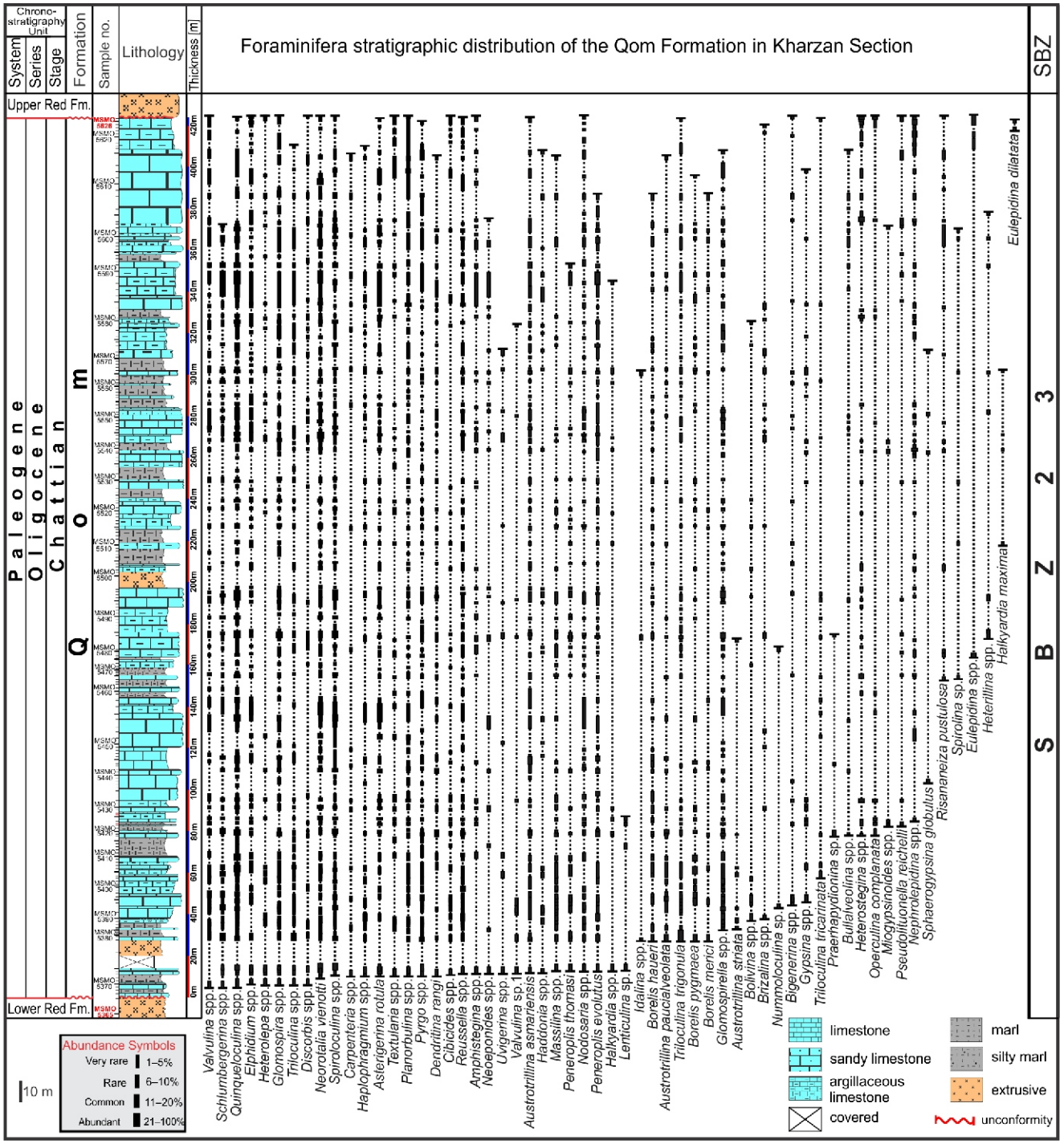

Fig. 4. Stratigraphic distribution chart of foraminifera in the Kharzan section studied

SBZ refers to a shallow benthic zone

A distribution chart displaying the foraminiferal assemblages from the Kharzan section is shown in Figure 4. The presence of *Miogypsinoides* spp. at 82 metres from the base of the section, and the association of this species with lepidocyclinids, *Heterostegina* spp., *Rizananeiza pustulosa* and *Operculina complanata,* without the presence of *Nummulites* almost to the end of the section, are interpreted to indicate the SBZ23 Biozone of Chattian age. High-resolution photographic images of some of the key foraminifera species present are shown in Figures 5 and 6. The geographical location of the stratigraphic sections adjacent to the Kharzan section referred to the Appendix 2 shown in Figure 1A.

MICROFACIES ANALYSIS

Based on the type and quantity of allochemical (skeletal and non-skeletal) and orthochemical contents, seven carbonate microfacies and marl or silty marl facies have been identified in the Qom Formation in the Kharzan section. They belong to three distinct depositional settings: lagoon, patch reef, and open marine (Fig. 7 and Appendix 3). Photomicrographs taken from each microfacies are displayed in Figures 8 and 9. Their description, sedimentary features, and structures are provided together with an interpretation of their depositional settings.

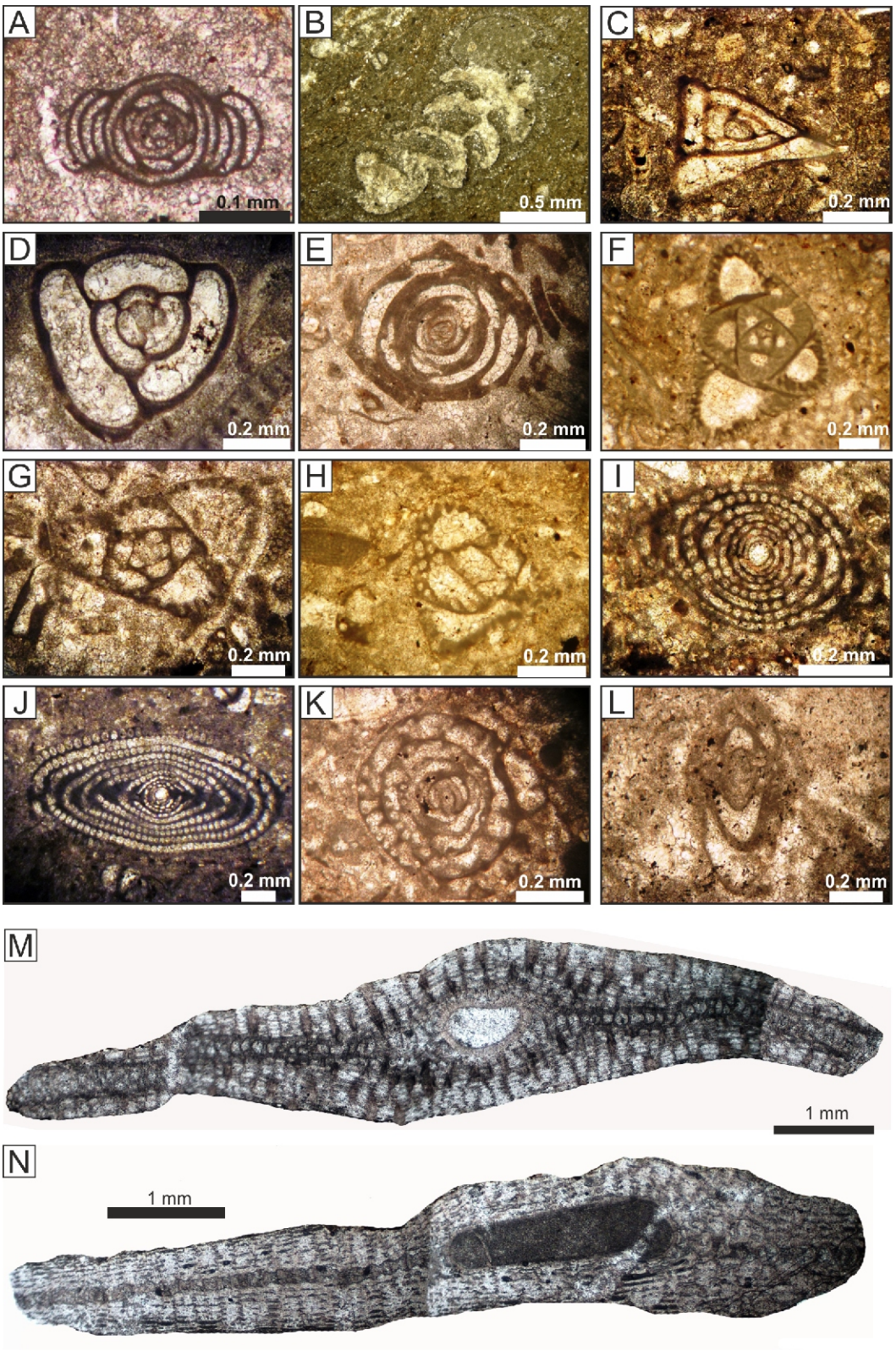

Fig. 5. Typical images of key foraminifera present in the Kharzan section studied

A – *Glomospirella* sp., sample no. MSMO 5450; **B** – *Haddonia* sp., sample no. MSMO 5389; **C** – *Triloculina tricarinata* d' Orbigny, 1826, sample no. MSMO 5584; **D** – *T.trigonula* d' Orbigny, 1826, sample no. MSMO 5566; **E** – *Idalina* sp., sample no. MSMO 5483; **F** – *Austrotrillina asmariensis* Adams, 1968, sample no. MSMO 5417; **G** – *A. paucialveolata* Grimsdale, 1952, sample no. MSMO 5418; **H** – *A. striata* Todd and Post, 1954, sample no. MSMO 5417; **I** – *Borelis merici* Sirel and Gunduz, 1981, sample no. MSMO 5510; **J** – *B. pygmaea* Hanzawa, 1930, sample no. MSMO 5405; **K** – *Bullalveolina* sp., sample no. MSMO 5597; **L** – *Dendritina rangi* d' Orbigny, *emend.* Fornasini, 1904, sample no. MSMO 5441; **M** – *Eulepidina dilatata* (Michelotti, 1861), sample no. MSMO 5625; **N** – *Eulepidina* sp., sample no. MSMO 5625

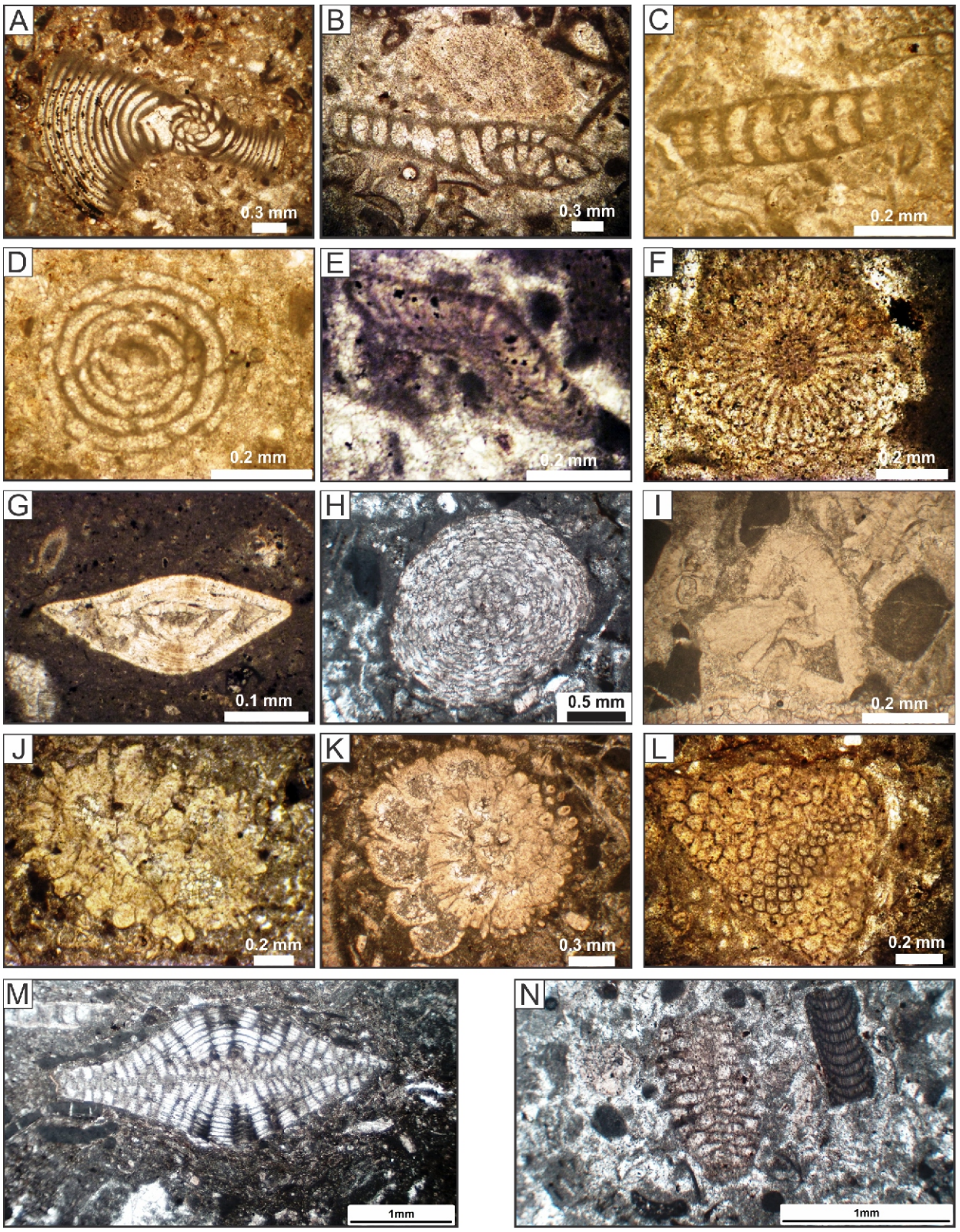

Fig. 6. Typical images of key foraminifera present in the Kharzan section studied

A – *P. evolutus* Henson, 1950, Sample no. MSMO 5483; **B** – *Peneroplis thomasi* Henson, 1950, Sample no. MSMO 5483; **C** – *Praerhapidionina* sp., sample no. MSMO 5418; **D** – *Borelis haueri* (Orbigny, 1846), sample no. MSMO, 5417; **E** – *Halkiyardia maxima* Cimmerman, 1969, sample no. MSMO 5529; **F** – *Halkiyardia* sp., sample no. MSMO 5539; **G** – *Asterigerina rotula* (Kaufmann), sample no. MSMO 5479; **H** – *Sphaerogypsina globulus* (Reuss, 1848), sample no. MSMO 5539; **I** – *Neorotalia vienotti* Greig, 1935, sample no. MSMO 5659 section; **J, K** – *Risananeiza pustulosa* Boukhary, Kuss and Abdelraouf, 2008: J – sample no. MSMO 5542; K – sample no. MSMO 5604; **L, N** – *Miogypsinoides* spp.: L – sample no. MSMO 5422, N – sample no. MSMO 5539; **M** – *Nephrolepidina* sp., sample no. MSMO 5621

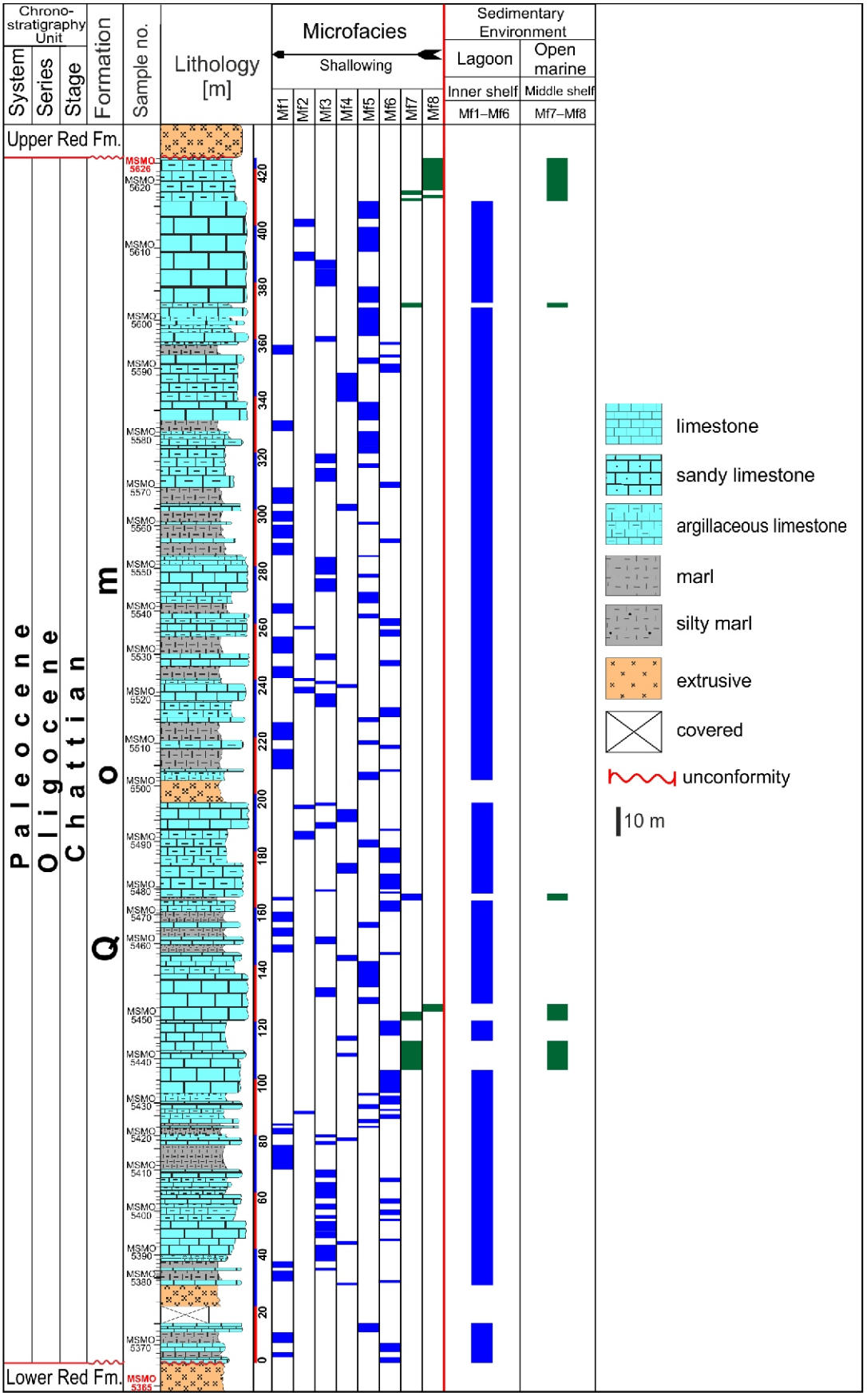

Fig. 7. Vertical microfacies distributions of the Qom Formation in the Kharzan section studied

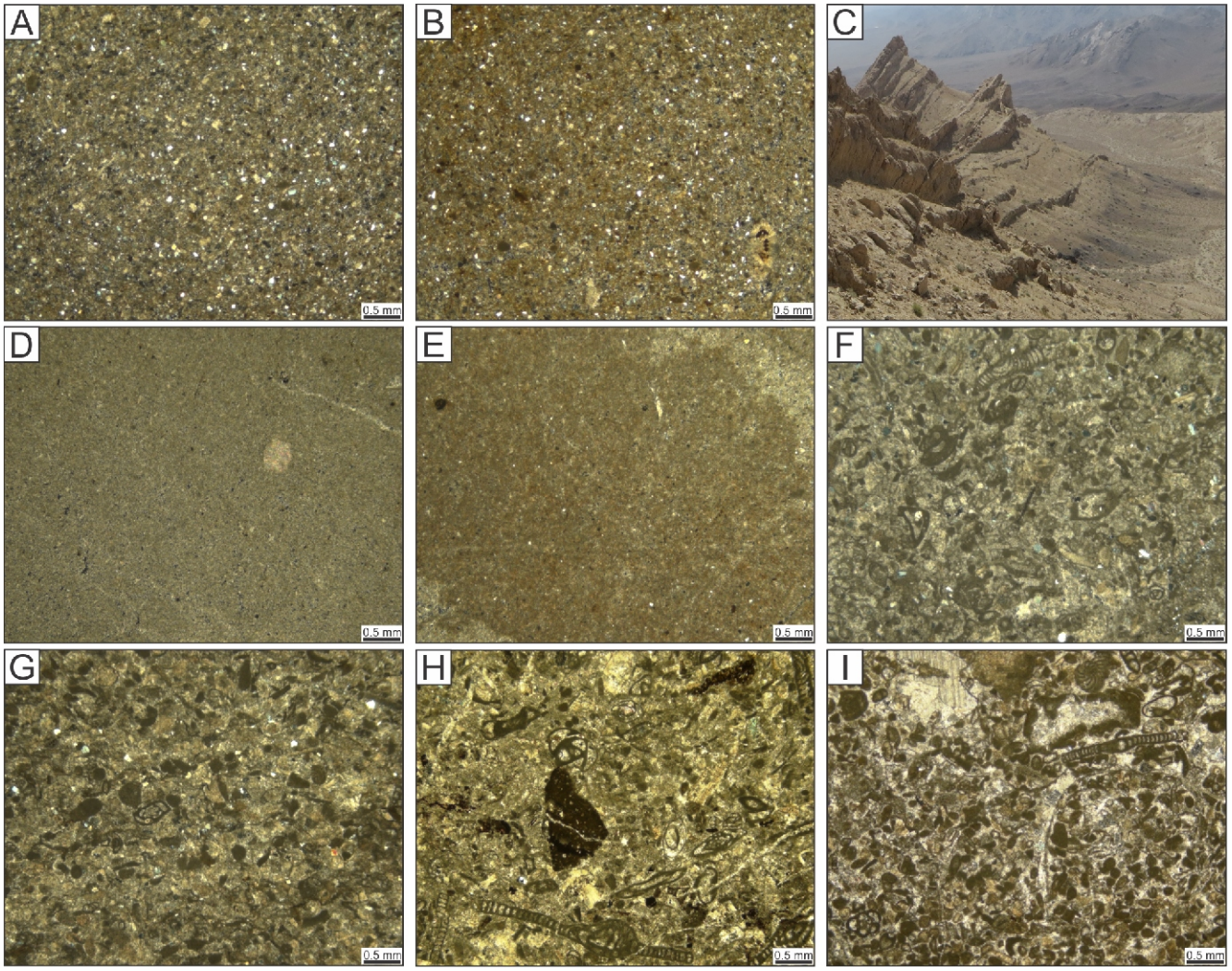

Fig. 8. A-C. Mf1: Silty marl A, B - Sample No. MSMO 5470, C. Alternations of marl or silty marl with limestone; Figs. D, E - Mf2: Silty mudstone D - Sample No. MSMO5593, E - Sample No. MSMO 5536; Figs. F, G - Mf3: Imperforate foraminiferal wackestone-packstone F - Sample No. MSMO 5375, G - Sample No. MSMO 5522; Figs. H, I - Mf4: Imperforate foraminiferal packstone- grainstone H - Sample No. MSMO 5601, I - Sample No. MSMO 5579

MF1: MARL OR SILTY MARL

This non-carbonate facies occurs almost throughout the succession studied, alternating with carbonate deposits. The biotic components of this facies are composed mainly of benthic foraminifera (miliolids) and ostracods (Fig. 8A–C).

Interpretation: Alternation of this facies with lagoonal microfacies (Mf2 and Mf3), together with the presence of ostracods and miliolids, suggest this facies was formed in a depositional environment with limited water circulation, such as a restricted lagoon.

MF2: SILTY MUDSTONE

Mf2 comprises a limy mudstone matrix with scattered silt-sized detrital quartz grains (Fig. 8D, E).

Interpretation: The lack of fossils in this microfacies is interpreted as an unfavourable environment for living organisms and/or for their preservation. The lack of structures related to periods of surface exposure, such as bird's-eye and mud cracks, may indicate a shallow, low-energy subaqueous protected environment (Wilson and Evans, 2002). In addition, the high percentage of mud and silt associated with this microfacies, and the position of these microfacies in the vertical sequence of the Qom Formation, indicate a lagoonal depositional environment, in part merging into a tidal flat setting (Geel, 2000; Flügel, 2010).

MF3: IMPERFORATE FORAMINIFERAL WACKESTONE-PACKSTONE

Mf3 consists mainly of porcellaneous foraminifera (miliolids, *Borelis, Dendritina, Austrotrillina, Peneroplis*) in a micritic matrix. It may also contain coralline red algae, echinoderms, agglutinated foraminifera, ostracods, gastropods and bivalves in lesser amounts. Some thin sections display the presence of sporadic quartz (10–15%) and are associated with a wackestone-packstone texture, indicating that Mf3 changes locally into a sandy bioclastic wackestone-packstone (Fig. 8F, G).

Interpretation: The presence of various imperforate benthic foraminifera and the absence of fossils with hyaline walls indicate a protected lagoon depositional environment (Romero et al., 2002). Also, a foraminifera assemblage with a predominance of miliolids may signify high-salinity shallow water with reduced water circulation, and limited oxygen content (Geel, 2000).

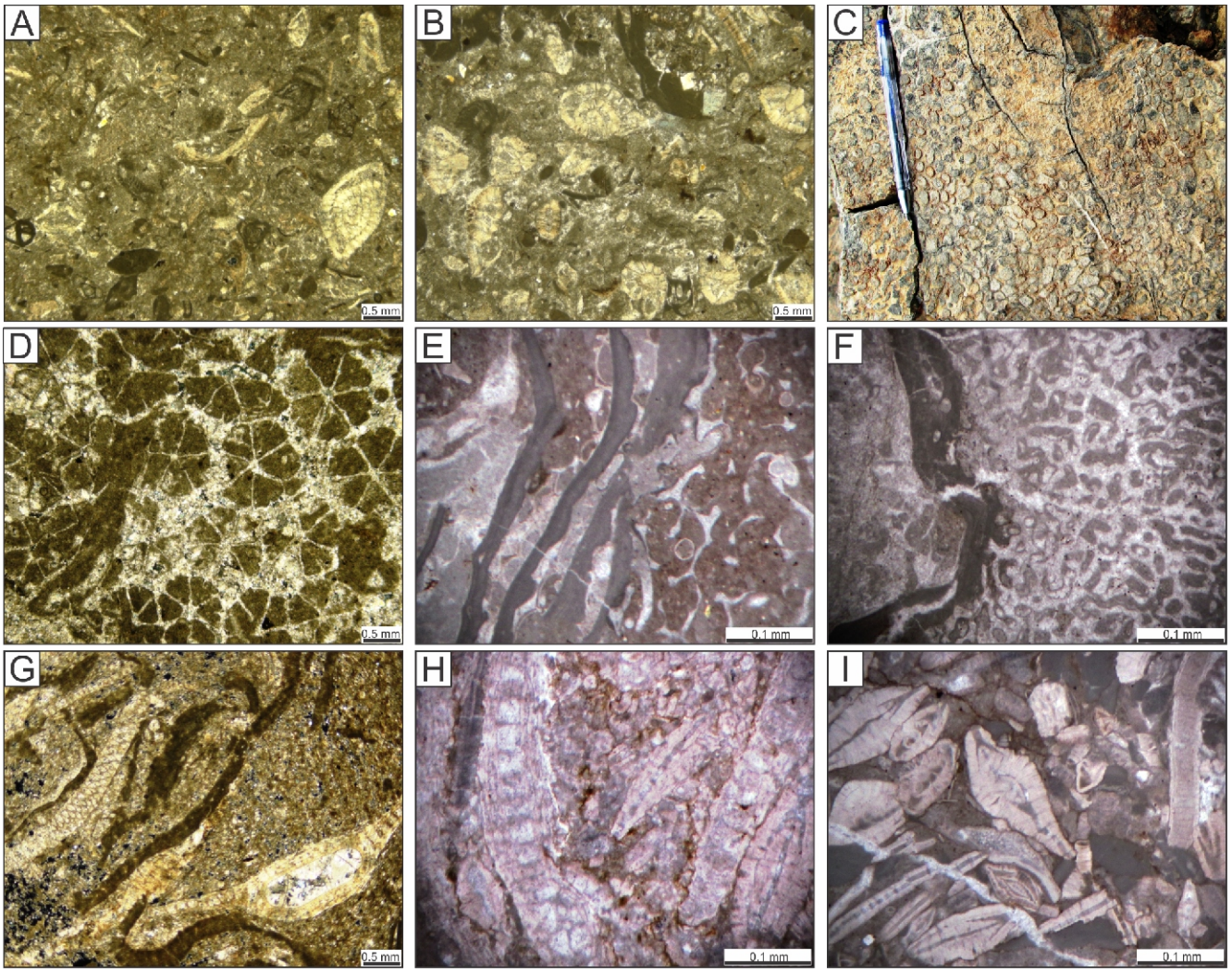

Fig. 9A, B – Mf5: red algal-foraminiferal packstone-grainstone: A – sample no. MSMO 5422, B – sample no. MSMO 5374; C, D – Mf6: coral boundstone, sample no. MSMO 5431; E, F – Mf7: coralline red algal-coral packstone-rudstone: E – sample no. MSMO 5723, F – sample no. MSMO 5438; G, H, I – Mf8: perforate foraminiferal wackestone-packstone: G – sample no. MSMO 5620, H – sample no. MSMO 5625, I – sample no. MSMO 5724

MF4: IMPERFORATE FORAMINIFERAL PACKSTONE-GRAINSTONE

Imperforate foraminifera such as miliolids, peneroplids and alveolinids are the main allochems in Mf4. Other components are red algal fragments, gastropods, bivalves, echinoids and foraminifera with agglutinated shells. With an increase in mud content, the microfacies changes into packstone. In some thin sections, the number of peloids and detrital quartz grains may reach 10% (Fig. 8H, I).

Interpretation: The high abundance of porcellaneous foraminifera indicates a hypersaline environment with limited water circulation (e.g., Geel, 2000). This microfacies represent a lagoonal depositional environment based on the standard microfacies classification of Flügel (2010).

MF5: RED ALGAL-FORAMINIFERAL PACKSTONE-GRAINSTONE

Mf5 consists mainly of hyaline-walled foraminifera (*Amphistegina, Neorotalia*, *Asterigerina*, and swollen and small Lepidocyclinidae, *Elphidium*), in association with imperforate foraminifera (miliolids) and coralline red algae fragments in a micritic matrix. Other components of this microfacies are bryozoans, coral, echinoderms, ostracods, gastropods, bivalves and agglutinated foraminifers. Due to the presence of allochems characteristic of more energetic depositional environments, such as bryozoans and colonial corals in a microcrystalline matrix, this microfacies is interpreted as most probably formed in the seaward parts of an open marine lagoon. Due to the lack of subaqueous shoals in the Kharzan section, the components of high-energy environments (such as reefs) are preserved as eroded fragments displaced into adjacent lagoonal depositional environments (Fig. 9A, B).

Interpretation: Due to the presence of allochems characteristic of more energetic depositional environments, such as bryozoans and fragmented parts of colonial corals in a microcrystalline matrix, this microfacies was most probably formed in the seaward parts of an open marine lagoon. Foraminifera with hyaline walls are usually present in normal marine salinity. Nevertheless, porcellaneous foraminifera also typically live in shallow-water environments with reduced water circulation, low oxygen levels, and high salinity (Geel, 2000). The presence of perforated and imperforate benthic foraminifera indicates deposition in shallow and semi-protected environments such as a lagoon (Geel, 2000; Romero et al., 2002; Vaziri-Moghaddam et al., 2006; Amirshahkarami et al.,

2007; and Mohammadi et al., 2019). The open marine lagoon is characterized by bioclastic rotaliids, miliolids and bioclast wackestone-packstone microfacies that include mixed open marine and restricted environment bioclasts (Vaziri-Moghaddam et al., 2010). The co-occurrence of normal marine biotas such as rotaliids, corallinaceans, and echinoids with lagoonal biota such as miliolids indicates that sedimentation took place in an open-shelf lagoon.

MF6: CORAL BOUNDSTONE

About 90% of microfacies Mf6 consist of intact and large colonial corals forming an organic rigid framework. In the spaces between the corals, lagoon-environment foraminifera (miliolids and *Borelis*) were observed. These corals occur discontinuously, making them difficult to trace over a long distance in the field (Fig. 9C, D).

Interpretation: Based on the standard microfacies proposed by Flügel (2010), the occurrence of in-situ organisms such as colonial corals suggests a reef environment. This Mf is interpreted as a reef, but based on its alternation with lagoonal microfacies (Mf4, Mf5) and field observations (discontinuous reefs occurring intermittently over long distances) these corals are related to patch reefs. This Mf is formed by *in situ* fauna as organic patch reefs formed in lagoon settings.

MF7: CORALLINE RED ALGAL-CORAL PACKSTONE-RUDSTONE

This Mf is characterized by abundant and densely packed skeletal grains. The most important constituents of microfacies Mf7 are red algae and corals. Hyaline-walled benthic foraminifers (*Amphistegina,* and *Lepidocyclina*), echinoderm fragments, bivalves and bryozoans are also present in lesser amounts (Fig. 9E, F). Coarse bioclasts, larger than 2 mm in size, are also present.

Interpretation: The association of corals and coralline red algae lead us to interpret a depositional environment for Mf7 involving substantial light and relatively high energy. The abundance of red algae suggests a depositional setting in front of reefs, plateaus, and ridges in a tropical sea (Okhravi and Amini, 1998; Pomar, 2001a). Flügel (2010) attributed this microfacies to the upper carbonate slope or the shallower part of a more open-marine and lower part of the reef belt (front of reef setting) depositional environment. Prevailing red algae and corals and the presence of LBFs, which are the most important components of Mf7, represent the preserved organisms that existed in this oligophotic zone (Pomar, 2001a, b; Brandano and Corda, 2002; Corda and Brandano, 2003). The accumulation of large bioclastic fragments removed from the reef with poor sorting indicates a depositional environment of relatively high energy associated with the lower part of the reef belt and/or the upper part of the slope.

MF8: PERFORATE FORAMINIFERAL WACKESTONE-PACKSTONE

Mf8 consists mainly of perforated-walled foraminifera, such as large and elongated Lepidocyclinidae (*Eulepidina*), *Heterostegina, Operculina*, *Neorotalia* and *Amphistegina*. The other constituents include bryozoans, fragments of echinoderms, ostracods, gastropods, bivalves and coralline red algae. Locally the size of Lepidocyclinidae exceeds the normal range, such that they are visible to the naked eye (Fig. 9G–I).

Interpretation: According to Hottinger (1983) and Pomar (2001a, b), the extensive presence of large and flat foraminifera such as Lepidocyclinidae, which are typically intact without any trace of fragmentation, together with Nummulitidae, may indicate an environment with normal oceanic salinity, towards the lower limits of the optical zone (Hallock and Glenn, 1986; Romero et al., 2002). Due to the reduction of turbulence at these greater depths, the foraminifera present tend to be deformed and have thinner shells. This is due to their slower growth tending to result in more elongated shell forms. Considering the high abundance of open marine fauna, such as Lepidocyclinidae and Nummulitidae, this microfacies was most likely deposited on the lower part of a carbonate slope (Geel, 2000). The abundance of red algae, and LBFs such as *Eulepidina, Neorotalia,* and *Operculina,* indicates that the depositional environment existed in the mesophotic to oligophotic zone (Pomar 2001a, b; Romero et al., 2002; Renema, 2006).

DISTRIBUTION OF FOSSIL ASSEMBLAGES AND DEPOSITIONAL ENVIRONMENTS IN THE SECTION STUDIED

The distribution and community of perforate and imperforate foraminifera, as well as the extents of terrestrial and carbonate facies, are the key factors that assist in defining a feasible sedimentary model for the Kharzan section. Continuous reefs, storm structures, and gravity-flow deposits (turbidites and debris flows), which are indicative of relatively rapid facies changes, are absent from the section studied. By comparing the interpreted microfacies of the Kharzan section with those described by Read et al., (1995), Pomar (2001a, b), and Flügel (2010), the sedimentary environment of the Qom Formation at this location is most likely an open carbonate shelf platform. A sedimentary model depicting the variations observed in that environment based on the samples studied is shown in Figure 10.

The inner shelf includes both lagoons and patch reefs, whereas the middle shelf comprises shallow-water environments existing in more open-marine conditions. The outer shelf environment has not been recognized in the outcrops of the Kharzan section. Inner shelf microfacies consist of Mf1, Mf2, Mf3, Mf4, Mf5 and Mf6. According to Hallock and Glenn (1986) and Geel (2000), imperforate foraminifera are abundant in the lagoonal environment. Miliolids, Dendritina, Peneroplis, Austrotrillina and Borelis are representatives of these taxa in the section studied. They are particularly abundant in microfacies Mf3 and Mf4.

Microfacies Mf1 and Mf2 were deposited on the shallowest inner shelf. The absence of any structures indicative of subaerial exposure such as mud cracks and bird's-eye structures) in Mf1, and its situation in the sedimentary sequence as a whole, indicates that it was deposited in a low-energy, shallow-water environment with limited water circulation: most probably a restricted lagoon similar to Mf2.

The most commonly identified microfacies representing the inner shelf are Mf3, Mf4, and Mf5. The imperforate foraminifera such as *Dendritina*, *Austrotrillina*, *Peneroplis*, *Borelis*, miliolids and textularids (microfacies Mf3-Mf4) also indicate lagoonal environments (Geel, 2000; Romero et al., 2002). A semi-restricted lagoon seems most likely due to the coexistence of a restricted marine fauna such as imperforate foraminifera and open marine fauna such as perforate foraminifera (microfacies Mf5). Microfacies Mf5 was observed to alternate with Mf6 in the section studied.

The co-ocurrence of an open-marine index species (perforated benthic foraminifera such as *Nephrolepidina* and *Amphistegina*, corallinaceans, bryozoans, and echinoids) with multiple lagoonal taxa (the imperforated benthic foraminifera such as miliolids, peneroplids and *Borelis*) in a generally lagoonal environment and also based on field observations (discontinuous and reefs untraceable over long distances) sug-

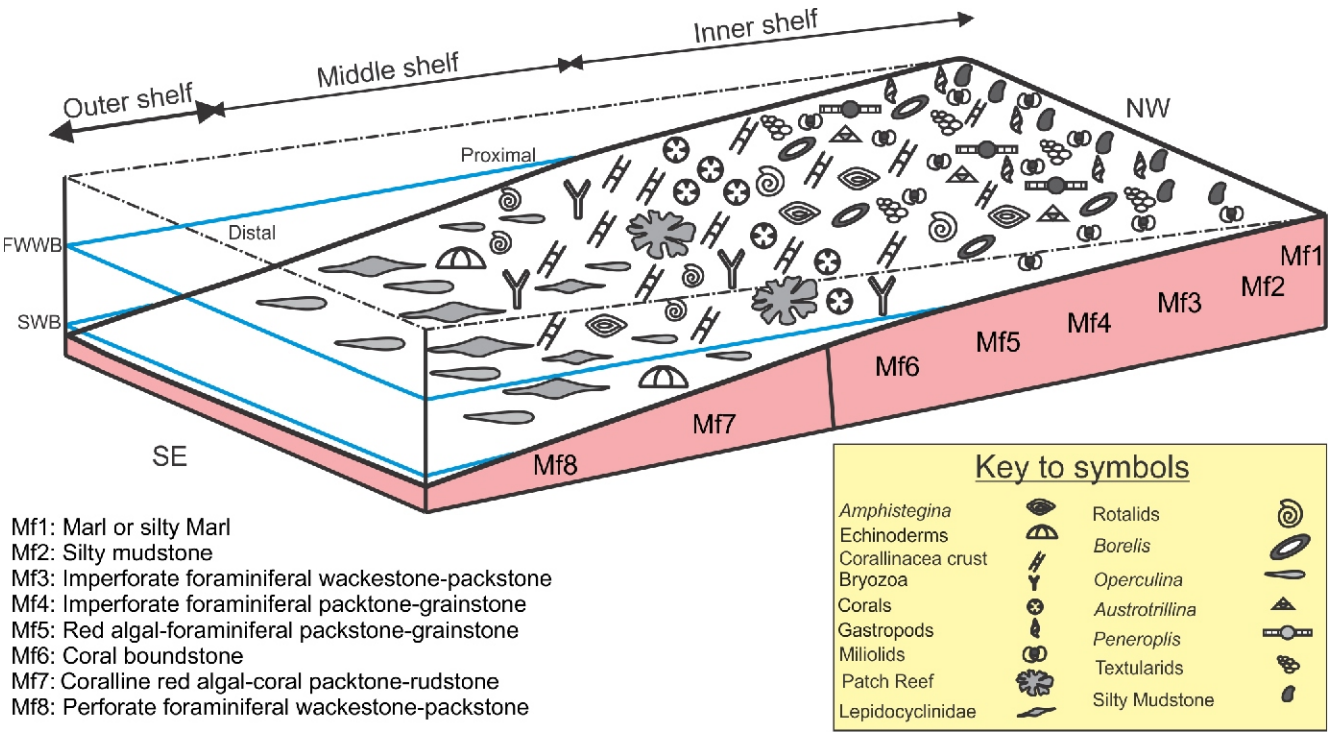

Fig. 10. Interpreted sedimentary environment model incorporating the distribution of microfacies observed in the Qom Formation exposed in the Kharzan section

See text for a detailed description of microfacies Mf1 to Mf8

gests the existence of a discontinuous reef system (i.e., patch reefs) in the Kharzan section. The middle-shelf microfacies include proximal and distal depositional environments. The proximal microfacies are characterized by the presence of reef-derived bioclasts such as colonial corals and coralline red algae in a packstone-rudstone fabric (microfacies Mf6 and Mf7). Mf7 is located in a shallower part of the middle shelf than Mf6. The middle shelf distal part includes perforate foraminifera, such as Lepidocyclinidae in microfacies Mf8. Perforate LBFs with symbiotic algae (e.g., Lepidocyclinidae and Nummulitidae in microfacies Mf8) are the major components in euphotic shallow water indicative of an open-marine depositional environment (Hallock and Glenn, 1986; Geel, 2000).

DIAGENETIC PROCESSES AND RESERVOIR QUALITY

Due to its diverse facies and microfacies types, the Qom Formation can act as source rock, reservoir rock and cap rock, providing all the components of an effective oil system (e.g., Rezaei and Honarmand, 2001). Two main factors of the sedimentary environment and diagenetic processes control its reservoir characteristics. The percentage and frequency of porosity, as well as changes in permeability, are the most basic and essential factors that determine a formation's reservoir quality. The most important diagenetic processes that have affected the limestone of the Qom Formation include micritization, cementation, mechanical and chemical compaction, dissolution, fracturing, and the vein-filling with calcite. In general, processes such as dissolution and fracturing have, at times, acted to improve the reservoir quality during the post-depositional history of the succession studied. On the other hand, the processes of micritization, cementation, compaction and calcite vein formation have subsequently acted to reduce the reservoir potential in much of the Qom Formation.

Secondary porosity such as of vuggy type (Fig. 11A) and fracture type (Fig. 11B) has been observed in the Kharzan section.

Compaction and cementation are two important processes that have acted to reduce porosity and permeability in the Qom Formation. The effects of compaction can be seen in the form of solution seams (Fig. 11C) and stylolites in the samples studied. Mechanical compaction (Fig. 11D) was observed within the mud-dominated facies of the Qom Formation, whereas chemical compaction dominates in the grain-based facies. The effects of physical compaction include the deformation of fossils and the break-up of bioclasts, especially lepidocyclinids and red algae. The effects of chemical compaction include stylolitization, dentate contacts between grains, and the formation of dissolution veins.

Cementation of the Qom Formation in the section studied occurs in the form of equant calcite, blocky, syntaxial overgrowths (Fig. 11E), drusy (Fig. 11F), mosaic (Fig. 11G), and pervasive anhydrite cements. Such types of cement have filled the intragranular pore space (Fig. 11H) as well as fractures and dissolution pores.

Pervasive anhydrite and coarsely crystalline gypsum cement also contribute to the deterioration of the reservoir quality of the Qom Formation. Cementation is most pervasive in the reef and the fore-reef facies. Additionally, micritization (Fig. 11I) was created by the activities of microorganisms, including cyanobacteria, algae, and fungi on the allochem surfaces (Garcia-Pichel, 2006). After the filling of pores and burrows with micrite, a micritic coat tends to develop around the rock and

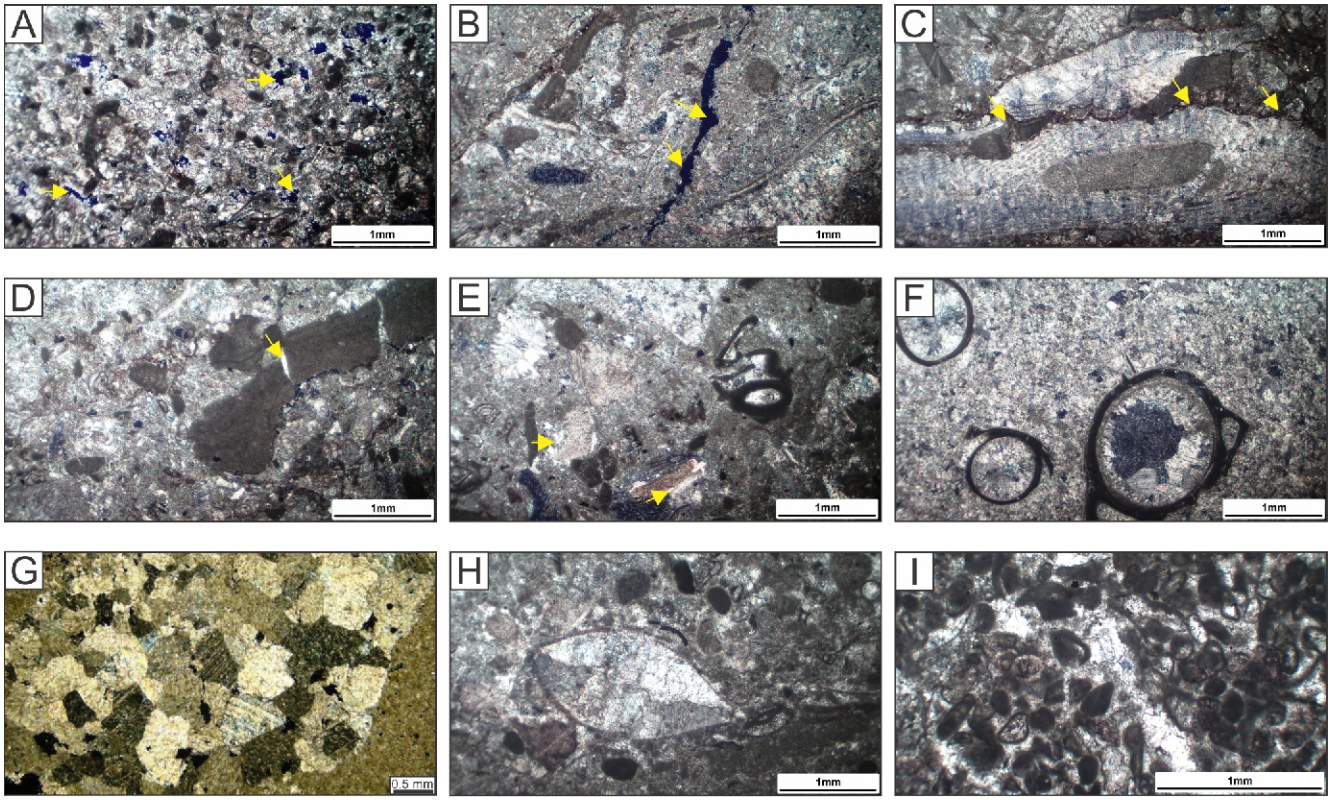

Fig. 11. Selected microscopic images of diagenetic processes in the Qom Formation

A – vuggy porosity; **B** – fracture porosity; **C** – solution seam; **D** – mechanical compaction; **E** – syntaxial overgrowth cement around echinoderm; **F** – drusy cement; **G** – calcite mosaic cement; **H** – bivalve interior filled with calcite; **I** – micritization

mineral particles that are present (e.g., Bathurst, 1975). The micritization process of the Qom Formation has led to a substantial reduction of connected porosity in certain zones.

The most important diagenetic processes that have increased the porosity and permeability of the carbonate sections of the Qom Formation are mineral dissolution and the development of fractures. The dissolution process leads primarily to the formation of vuggy porosity, which is mainly observed in the restricted lagoon facies, particularly in the shallow parts of the inner shelf, which were more exposed to sea-level changes. Fractures are widely observed in this formation, and when first formed they substantially increased permeability, but many of those fractures are now filled (partly or completely) with sparitic calcite cement, which decreased their ability to positively impact the permeability of the formation. Diagenetic processes are the most important factors controlling porosity and permeability in the Qom Formation. However, a substantial part of the diagenetic processes observed, especially dissolution and cementation, occurred shortly after deposition and during early diagenesis. Consequently, these reservoir parameters display a close relationship with sedimentary facies, and thus the sedimentary environment affects porosity and permeability. The porosity that exists in marl and marly limestones is microporosity, whereas packstone-grainstone facies have vuggy porosity. Due to diagenetic processes such as compaction and intense cementation in the reef and packstone facies in the fore-reef environment, these facies display low reservoir quality. The occurrence of various diagenetic processes has acted to reduce porosity in much of the Qom Formation. In addition to primary cementation, the diagenetic processes observed include secondary cementation, anhydritization, compaction, micritization and veins filled with calcite cement. In the area studied, the limestone layers of this formation tend not to retain much primary porosity. Secondary porosity development processes are not widespread in this formation, being restricted to the shallow lagoonal facies, although most of the facies of the Qom Formation present in the section studied are fine-grained, mud-supported, carbonate lithologies with relatively poor primary porosity. Some of the mud-supported deposits have been beneficially affected by diagenetic processes, particularly dissolution and fracturing, leading to zones within the formation with improved reservoir quality.

CONCLUSIONS

Biogenic components of the Qom Formation in the Kharzan section in the north-west of Ardestan are dominated by large benthic foraminifera (LBF), hyaline, and porcellaneous and agglutinated benthic foraminifera, corals, and coralline red algae. The distribution of LBF in the studied area makes it possible to correlate the microfossil assemblages of central Iran with the standard shallow benthic zonation (SBZ) of the European Basin. Lipidocyclinidae and Miogypsinidae zonal markers in the Qom Formation show a good correlation with SBZ23, which indicates its late Oligocene (Chattian) age. Facies analysis based on field observation and petrographic data facilitates the recognition of eight microfacies varying between lagoon (Mf1–Mf5), patch reef (Mf6), and slope (Mf7, Mf8) environments. These identified microfacies and the dispersion of micro-organisms within them suggest an open-shelf depositional environment for the Qom Formation in the study area. In detail, that environment

comprises inner and middle (proximal and distal) shelf components. Microfacies Mf1-Mf6 represent the middle shelf and Mf7, and Mf8 represents the inner shelf.

Study of the carbonate strata of the Qom Formation revealed that cementation occurred widely throughout these strata. Cementation has destroyed a large amount of the primary and secondary porosity, and thereby substantially degraded reservoir quality. Although dissolution and fracturing created extensive secondary porosity, the fractures and vuggy porosity formed have for the most part been subsequently filled with cement, leading to a deterioration in reservoir quality. Micritization and compaction have also contributed to a post-depositional reduction in the formation's porosity Moreover, in some zones, chemical compaction has created stylolites. In general, zones associated with shallow lagoonal facies display better reservoir quality than other facies due to the greater influence and preservation of dissolution zones and fractures. Fracturing is a consequence of post-depositional active regional tectonic movements caused by volcanic episodes and horst and graben development. Overall, diagenetic processes have substantially affected the Qom Formation in the section studied, degrading its reservoir quality, but some shallow-lagoonal facies zones remain with viable reservoir quality.

Acknowledgements. This project was funded by the Ferdowsi University of Mashhad (grant number 3/44368 to A.AA.). The authors are grateful to the National Iranian Oil Company Exploration Directorate for providing samples and thin sections and the Ferdowsi University of Mashhad for their logistical support during the study. We also thank Dr. Mohammad Reza Arianasab from the National Iranian Oil Company, Exploration Directorate for his helpful comments on the manuscript. Two referees are acknowledged for their insightful reviews, constructive comments and useful remarks.

REFERENCES

Adams, C.G., Belford, D.J., 1974. Foraminiferal Biostratigraphy of the Oligocene–Miocene Limestones of Christmas Island (Indian Ocean), Paleontology, **1**: 475–506.

Adams, C.G., Gentry, A.W., Whybrow, P.J., 1983. Dating the terminal Tethyan event. Utrecht Micropaleontological Bulletins, **30**: 273–298.

Adams, T.D., Bourgeois, F., 1967. Asmari biostratigraphy Iran. Iranian Oil Operating Companies Geological and Exploration Division, **1074**: 1–37.

Agard, P., Omrani, J., Jolivet, L., Whitechurch, H., Vrielynck, B., Spakman, W., Monie, P., Meyer, B., Wortel, R., 2011. Zagros orogeny: a subduction-dominated process. Geological Magazine, **148**: 692–725; https://doi.org/10.1017/S001675681100046X

Akbar-Baskalayeh, N., Less, G., Ghasemi-Nejad, E., Yazdi-Moghadam, M., Pignatti, J., 2020. Biometric study of late Oligocene larger benthic Foraminifera (Lepidocyclinidae and Nummulitidae) from the Qom Formation, Central Iran (Tajar-Kuh section). Journal of Paleontology, **94**: 593–615; https://doi.org/10.1017/jpa.2020.5

Allahkarampour Dill, M., Vaziri-Moghaddam, H., Seyrafian, A., Behdad, A., 2018. Oligo-Miocene carbonate platform evolution in the northern margin of the Asmari intra-shelf basin, SW Iran. Marine and Petroleum Geology, **92**, 437–461; https://doi.org/10.1016/j.marpetgeo.2017.11.008

Amirshahkarami, M., Karavan, M., 2015. Microfacies models and sequence stratigraphic architecture of the Oligocene–Miocene Qom Formation, south of Qom City, Iran. Geoscience Frontiers, **6**: 593–604; https://doi.org/10.1016/j.gsf.2014.08.004

Amirshahkarami, M., Vaziri-Moghaddam, H., Taheri, A., 2007. Sedimentary facies and sequence stratigraphy of the Asmari Formation at Chaman-Bolbol, Zagros Basin, Iran. Journal of Asian Earth Sciences, **29**: 947–959; https://doi.org/10.1016/j.jseaes.2006.06.008

Amirshahkarami, M., Ghabishavi, A., Rahmani, A., 2010. Biostratigraphy and paleoenvironment of the larger benthic foraminifera in wells sections of the Asmari Formation from the Rag-e-Safid oil field, Zagros Basin, southwest Iran. Zagros Basin, southwest Iran. Stratigraphy and Sedimentology Researches, **40**: 63–48.

Baghbani, D., Alahiari, M., Shakeri, A., 1996. Investigation of Sediment Basin, Hydrocarbon Capacity, Stratigraphy, Sedimentary Cycles, Active Faults of Tectonic, Sediment Area and Palaeogeography of the Qom Formation, Project of National Iranian Oil Company (in Persian).

Barattolo, F., Bassi, D., Romano, R., 2007. Upper Eocene larger foraminiferal-coralline algal facies from the Klokova Mountain (southern continental Greece). Facies, **53**: 361–375; https://doi.org/10.1007/s10347-007-0108-2

Bassi, D., Hottinger, L., Nebelsick, J.H., 2007. Larger foraminifera from the Upper Oligocene of the Venetian area, northeast Italy. Paleontology, **50**: 845–868; https://doi.org/10.1111/j.1475-4983.2007.00677.x

Basso, D., Coletti, G., Bracchi, V.A., Yazdi-Moghadam, M., 2019. Lower Oligocene coralline algae of the Uromieh section (Qom Formation, NW Iran) and the oldest record of Titanoderma pustulatum (Corallinophycidae, Rhodophyta). Rivista Italiana di Paleontologia e Stratigrafia, **125**: 197–218; https://doi.org/.13130/2039-4942/11382

Bathurst, R.G.C., 1975. Carbonate Sediments and their Diagenesis. Developments in Sedimentology, **12**.

Beavington-Penney, S.J., Racey, A., 2004. Ecology of extant nummulitids and other larger benthic foraminifera: applications in palaeoenvironmental analysis. Earth-Science Reviews, **67**: 219–265; https://doi.org/10.1016/j.earscirev.2004.02.005

Behforouzi, E., Safari, A., 2011. Biostratigraphy and paleoecology of the Qom Formation in Chenar area (northwestern Kashan), Iran. Revista Mexicana de Ciencias Geológicas, **28**: 555–565.

Bellen, R.C. Van. M., Dunnington., H.V., Wetyzel, R., Morton, D., 1959. Lexique stratigraphique, International. Asia, Iraq, **3**: 1–333.

Bozorgnia, F., 1966. Qum Formation stratigraphy of the Central Basin of Iran and its intercontinental position. Bulletin of the Iranian Petroleum Institute, **24**: 69–75.

Bozorgnia, F., Kalantari, A, 1965. Nummulites of Parts of Central and East Iran. (A Thin-section Study). National Iranian Oil Company, Tehran.

Brandano, M., Corda, L., 2002. Nutrients, sea level, and tectonics: constraints for the facies architecture of a Miocene carbonate ramp in central Italy. Terra Nova, **14**: 257–262; https://doi.org/10.1046/j.1365-3121.2000.00419.x

Cahuzac, B., Poignant, A., 1997. Essai de biozonation de l'Oligo-Miocène dans les bassins européens á l'aide des grands foraminifères néritiques. Bulletin de la Société géologique de France, **168**: 155–169.

Corda, L., Brandano, M., 2003. Aphotic zone carbonate production on a Miocene ramp, Central Apennines, Italy. Sedimentary Geology, **161**: 55–70; https://doi.org/10.1016/S0037-0738(02)00395-0

Ćosović, V., Drobne, K., Moro, A., 2004. Paleoenvironmental model for Eocene foraminiferal limestones of the Adriatic carbonate platform (Istrian Peninsula). Facies, **50**: 61–75; https://doi.org/10.1007/s10347-004-0006-9

Daneshian, J., Dana, L.R., 2007. Early Miocene benthic foraminifera and biostratigraphy of Qom Formation, Deh Namak, Central Iran. Journal of Asian Earth Sciences, **29**: 844–858; https://doi.org/10.1016/j.jseaes.2006.06.003

Daneshian, J., Dana, L.R., 2019. Benthic foraminiferal events of the Qom Formation in the North Central Iran Zone. Paleontological Research, **23**: 10–22; https://doi.org/10.2517/2018PR008

Daneshian, J., Ghanbari, M., 2017. Stratigraphic distribution of planktonic foraminifera from the Qom Formation: a case study from the Zanjan area (NW Central Iran). Neues Jahrbuch für Geologie und Paläontologie Abhandlungen, **283**: 239–254; https://doi.org/10.1127/njgpa/2017/0636

Daneshian, J., Dana, L.R., Sadler, P., 2017. A composite foraminiferal biostratigraphic sequence for the Lower Miocene deposits in the type area of the Qom Formation, central Iran, developed by constrained optimization (CONOP). Journal of African Earth Sciences, **125**: 214–229; https://doi.org/10.1016/j.jafrearsci.2016.09.023

Deighton, I., 1985. Foraminifera biostratigraphy general report. In: Area Report East Iran Project Are No. 1 (North and South Baluchestan) (ed. G. J. H. McCall). Geological Survey of Iran, Ministry of Mine and Metals.

Dill, M.A., Vaziri-Moghaddam, H., Seyrafian, A., Behdad, A., Shabafrooz, R., 2020. A review of the Oligo-Miocene larger benthic foraminifera in the Zagros basin, Iran; New insights into biozonation and palaeogeographical maps. Revue de Micropaléontologie, **66**, 100408; https://doi.org/org/10.1016/j.revmic.2020.100408

Dunham, R.J., 1962. Classification of carbonate rocks according to depositional texture. AAPG Memoir, **1**: 80–121.

Ehrenberg, S.N., Pickard, N.A.H., Laursen, G.V., Monibi, S., Mossadegh, Z.K., Svana, T.A., Aqrawi, A.A.M., McArthur, J.M., Thirlwall, M.F., 2007. Strontium isotope stratigraphy of the Asmari Formation (Oligocene Lower Miocene), SW Iran. Journal of Petroleum Geology, **30**: 107–128; https://doi.org/10.1111/j.1747-5457.2007.00107.x

Embry, A.F., Klovan, J.E., 1971. A late Devonian reef tract on northeastern Banks Island, NWT. Bulletin of Canadian Petroleum Geology, **19**: 730–781.

Flügel, E., 2010. Microfacies of Carbonate Rocks, Analysis, Interpretation and Application. Springer, Berlin.

Garcia-Pichel, F., 2006. Plausible mechanisms for the boring of carbonates by microbial phototrophs. Sedimentary Geology, **185**: 205–213; https://doi.org/10.1016/j.sedgeo.2005.12.013

Geel, T., 2000. Recognition of stratigraphic sequences in carbonate platform and slope deposits: empirical models based on microfacies analysis of Palaeogene deposits in southeastern Spain. Palaeogeography, Palaeoclimatology, Palaeoecology, **155**: 211–238; https://doi.org/10.1016/S0031-0182(99)00117-0

Hadavi, F., Moghaddam, M. M. and Mousazadeh, H., 2010. Burdigalian-Serravalian calcareous nannoplanktons from Qom Formation, North-Center Iran. Arabian Journal of Geoscience, **3**: 133–139.

Hallock, P., Glenn, E.C., 1986. Larger foraminifera: a tool for paleoenvironmental analysis of Cenozoic carbonate depositional facies. Palaeogeography, Palaeoclimatology, Palaeoecology, **1**: 44–64; https://doi.org/10.2307/3514459

Harzhauser, M., Piller, W.E., 2007. Benchmark data of a changing sea-paleogeography, palaeobiogeography, and events in the Central Paratethys during the Miocene. Palaeogeography, Palaeoclimatology, Palaeoecology, **253**: 8–31; https://doi.org/10.1016/j.palaeo.2007.03.031

Hottinger, L., 1983. Processes determining the distribution of larger foraminifera in space and time. Utrecht Micropaleontological Bulletins, **30**: 239–253.

Jones, R.W., Racey, A., Simmons, M.D., 1994. Cenozoic stratigraphy of the Arabian Peninsula and Gulf. Micropalaeontology and Hydrocarbon Exploration in the Middle East: 273–307. Chapman and Hall, London.

Kalantari, A, 1976. Microbiostratigraphy of the Sarvestan area, Southwestern Iran (Geological Laboratories Publication No.5). National Iranian Oil Company, Tehran.

Karavan, M., Vaziri-Moghaddam, H., Mahboubi, A., Moussavi-Harami, R., 2014. Biostratigraphy and paleo-ecological reconstruction on scleractinian reef corals of Rupelian-Chattian succession (Qom Formation) in the northeast of Delijan area. Geopersia, **4**: 11–24.

Khaksar, K., Moghadam, I.M., 2007. Paleontological study of the echinoderms in the Qom Formation (Central Iran). Earth Science Research Journal, **11**: 57–79.

Laursen, G. V., Monibi, S., Allan, T. L., Pickard, N. A. H., Hosseiney, A., Vincent, B., Hamon, Y., Van Buchem, F. S. P., Moallemi, A., Druillion, G., 2009. The Asmari Formation revisited: changed stratigraphic allocation and new biozonation. First International Petroleum Conference and Exhibition Shiraz, Iran.

Mohammadi, E., 2022. Foraminiferal biozonation, biostratigraphy, and trans-basinal correlation of the Oligo-Miocene Qom Formation, Iran (northeastern margin of the Tethyan Seaway). Palaeoworld (in press, corrected proof); https://doi.org/10.1016/j.palwor.2022.04.005

Mohammadi, E., Ameri, H., 2015. Biotic components and biostratigraphy of the Qom Formation in northern Abadeh, Sanandaj-Sirjan fore-arc basin, Iran (northeastern margin of the Tethyan Seaway). Arabian Journal of Geosciences, **8**: 10789–10802.

Mohammadi, E., Safari, A., Vaziri-Moghaddam, H., Vaziri, M.R., Ghaedi, M., 2011. Microfacies analysis and paleoenvironmental interpretation of the Qom Formation, south of the Kashan, Central Iran. Carbonates and Evaporites, **26**: 255–271; https://doi.org/ 10.1007/s13146-011-0059-0

Mohammadi, E., Hasanzadeh-Dastgerdi, M., Ghaedi, M., Dehghan, R., Safari, A., Vaziri-Moghaddam, H., Baizidi, C., Vaziri, M., Sefidari, E., 2013. The Tethyan Seaway Iranian Plate Oligo-Miocene deposits (the Qom Formation): distribution of Rupelian (early Oligocene) and evaporite deposits as evidence for the timing and trending of opening and closure of the Tethyan Seaway. Carbonates and Evaporites, **28**: 321–345; https://doi.org/ 10.2517/2018PR008

Mohammadi, E., Vaziri, M.R., Dastanpour, M., 2015. Biostratigraphy of the nummulitids and lepidocyclinids bearing Qom Formation based on larger benthic foraminifera (Sanandaj-Sirjan fore-arc basin and Central Iran back-arc basin, Iran). Arabian Journal of Geosciences, **8**: 403–423.

Mohammadi, E., Hasanzadeh-Dastgerdi, M., Safari, A., Vaziri-Moghaddam, H., 2019. Microfacies and depositional environments of the Qom Formation in Barzok area, SW Kashan, Iran. Carbonates and Evaporites, **34**: 1293–1306; https://doi.org/ 10.1007/s13146-017-0415-9

Murray, J.W., 2006. Ecology and Applications of Benthic Foraminifera. Cambridge University Press.

Nayebi, Z., 1995. Microbiostratigraphy of the Qom Formation in Kamarkuh and Dobaradar areas (in Persian). M.Sc. Thesis, Shahid Beheshti University.

Nebelsick, J.H., Stingl, V., Rasser, M., 2001. Autochthonous facies and allochthonous debris flows compared: Early Oligocene carbonate facies patterns of the Lower Inn Valley (Tyrol, Austria). Facies, **44**: 31–46; https://doi.org/10.1007/BF02668165

Nouradini, M., Azami, H. R., Hamed, M., Yazdi, M., 2015. Foraminiferal paleoecology and paleoenvironmental reconstructions of the lower Miocene deposits of the Qom Formation in Northeastern Isfahan, Central Iran. Boletin de la Sociedad Geológica Mexicana, **67**: 59–73; https://doi.org/10.18268/BSGM2015v67n1a5

Okhravi, R., Amini, A., 1998. An example of mixed carbonate-pyroclastic sedimentation (Miocene, Central Basin, Iran). Sedimentology, **118**: 37–54; https://doi.org/10.1016/S0037-0738(98)00004-9

Parandavar, M., Hadavi, F., 2019. Identification of the Oligocene-Miocene boundary in the Central Iran Basin (Qom Formation): calcareous nannofossil evidence. Geological Quarterly, **63** (2): 215–229; https://doi.org/10.7306/gq.1464

Pomar, L., 2001a. Ecological control of sedimentary accommodation: evolution from a carbonate ramp to rimmed shelf, Upper Miocene, Balearic Islands. Palaeogeography, Palaeoclimatology, Palaeoecology, **175**: 249–272; https://doi.org/10.1016/S0031-0182(01)00375-3

Pomar, L., 2001b. Types of carbonate platforms: a genetic approach. Basin Research, **13**: 313–334; https://doi.org/10.1046/j.0950-091x.2001.00152.x

Racey, A., 1994. Biostratigraphy and palaeobiogeographic significance of Tertiary nummulitids (foraminifera) from northern Oman. Micropalaeontology and Hydrocarbon Exploration in the Middle East: 343–367.

Radfar, J., Amini, B., 1999. Geological map of Iran, Ardestan, sheet no. 6457, scale 1:100,000. Geological Survey of Iran.

Rahaghi, A., 1980. Tertiary faunal assemblage of Qum-Kashan, Sabzewar, and Jahrum area. National Iranian Oil Company, Geological Laboratories, **8**: 1–64.

Rasser, M.W., Nebelsick, J.H., 2003. Provenance analysis of Oligocene autochthonous and allochthonous coralline algae: a quantitative approach towards reconstructing transported assemblages. Palaeogeography, Palaeoclimatology, Palaeoecology, **201**: 89–111; https://doi.org/10.1016/S0031-0182(03)00512-1

Read, J.F., Kerans, C., Weber, L.J., Sarg, J.F., Wright, F.M., 1995. Milankovitch sea-level changes, cycles and reservoirs on carbonate platforms in greenhouse and ice-house worlds. SEPM Short Course Notes, **35**, pt. 1.

Renema, W., 2006. Large benthic foraminifera from the deep photic zone of a mixed siliciclastic-carbonate shelf off East Kalimantan, Indonesia. Marine Micropaleontology, **58**: 73–82; https://doi.org/10.1016/j.marmicro.2005.10.004

Reuter, M., Piller, W.E., Harzhauser, M., Mandic, O., Berning, B., Rogl, F., Kroh, A., Aubry, M.P., Wielandt-Schuster, U., Hamedani, A., 2009. The Oligo-/Miocene Qom Formation (Iran): evidence for an early Burdigalian restriction of Tethyan Seaway and closure of its Iranian gateways. International Journal of Earth Sciences, **98**: 627–650; https://doi.org/10.1007/s00531-007-0269-9

Rezaei, M. R., Honarmand, J., 2001. Controller parameters the reservoir quality of Qom Formation in Alborz field, Qom basin, Central Iran (in Persian). Tehran University Science Journal, **27** (1–6).

Romero, J., Caus, E., Rossel, J., 2002. A model for the Palaeoenvironmental, distribution of larger foraminifera based on late middle Eocene deposits on the margin of the south Pyrenean Basin (SE Spain). Palaeogeography, Palaeoclimatology, Palaeoecology, **179**: 43–56; https://doi.org/10.1016/S0031-0182(01)00406-0

Sartorio, D., Venturini, S., 1988. Southern Tethys Biofacies. Agip Stratigraphic Department.

Schuster, F., Wielandt, U., 1999. Oligocene and early Miocene coral faunas from Iran: paleoecology and paleobiogeography. International Journal of Earth Sciences, **88**: 571–581; https://doi.org/ 10.1007/s005310050285

Seddighi, M., Vaziri-Moghaddam, H., Taheri, A., Ghabeishavi, A., 2012. Depositional environment and constraining factors on the facies architecture of the Qom Formation, Central Basin, Iran. Historical Biology, **24**: 91–100; https://doi.org/10.1080/08912963.2011.580434

Serra-Kiel, J., Martin-Martin, M., El Mamoune, B., Martin-Algarra, A., Martin-Perez, J.A., Tosquella, J., Frrandez-Canadell, C., Serrano, Y.F., 1998. Bioestratigraphia y lithostratigraphic del Paleogeno del area de Sierra Espuna (Cordillera Betica Oriental, SE de Espana). Acta Geológica Hispanica, **31**: 161–189.

Seyrafian, A., Torabi, H., 2005. Petrofacies and sequence stratigraphy of the Qom Formation (late Oligocene-early Miocene?), north of Nain, a southern trend of the Central Iranian Basin. Carbonates and Evaporites, **20**: 82–90; https://doi.org/10.1007/bf03175451

Stocklin, J., Setudehnia, A., 1991. Stratigraphic Lexicon of Iran Ministry of Industry and Mines. Geological Survey of Iran, **18**: 1–376.

Taheri, M.R., Vaziri-Mogaddam, H., Taheri, A., Ghabeishavi, A., 2017. Biostratigraphy and paleoecology of the oligo-Miocene Asmari formation in the Izeh zone (Zagros Basin, SW Iran). Boletín de la Sociedad Geológica Mexicana, **69**: 59–85; https://doi.org/10.18268/BSGM2017v69n1a4

Van Buchem, F.S.P., Allan, T.L., Laursen, G.V., Lotfpour, M., Moallemi, A., Monibi, S., Motei, H., Pickard, N.A.H., Tahmasbi, A.R., Vedvenne, V., Vincent, B., 2010. Regional stratigraphic architecture and reservoir types of the Oligo-Miocene deposits in the Dezful Embayment (Asmari and Pabdeh Formations) SW Iran. Geological Society Special Publications, **329**: 219–263; https://doi.org/10.1144/SP329.10

Vaziri-Moghaddam, H., Kimiagari, M.,Taheri, A., 2006. Depositional environment and sequence stratigraphy of the Oligo-Miocene Asmari Formation in SW Iran. Facies, **52**: 41–51; https://doi.org/10.1007/s10347-005-0018-0

Vaziri-Moghaddam, H., Seyrafian, A., Taheri, A., Motiei, H., 2010. Oligocene-Miocene ramp system (Asmari Formation) in the NW of the Zagros basin, Iran: Microfacies, paleoenvironment, and depositional sequence. Revista Mexicana de Ciencias Geológicas, **27**: 56–71.

Wilson, M.E., Evans, M.J., 2002. Sedimentology and diagenesis of Tertiary carbonates on the Mangkalihat Peninsula, Borneo: implications for subsurface reservoir quality. Marine and Petroleum Geology, **19**: 873–900; https://doi.org/10.1016/S0264-8172(02)00085-5

Wynd, J.G., 1965. Biofacies of the Iranian Oil Consortium Agreement Area. Iranian Oil Operating Companies Geological and Exploration division. Report no. 1082.

Yazdi-Moghadam, M., Sadeghi, A., Adabi, M.H., Tahmasbi, A., 2018. Foraminiferal biostratigraphy of the lower Miocene Hamzian and Arashtanab sections (NW Iran), northern margin of the Tethyan Seaway. Geobios, **51**: 231–246; https://doi.org/10.1016/j.geobios.2018.04.008

Yazdi-Moghadam, M., Sadeghi, A., Adabi, M.H., Tahmasbi, A., 2018. Stratigraphy of the lower Oligocene nummulitic limestones, north of Sonqor (NW Iran). Rivista Italiana di Paleontologia e Stratigrafia, **124**.

Yazdi-Moghadam, M., 2011. Early Oligocene larger foraminiferal biostratigraphy of the Qom Formation, South of Uromieh (NW Iran). Turkish Journal of Earth Science, **20**: 847–856.

https://www.Iranview.com. 2020

APPENDIX 1

Qom Formation benthic foraminifera identified in the Kharzan Section

Amphistegina spp., *Asterigerina rotula* (Kaufmann)*, Austrotrillina asmariensis* Adams, 1968*, A. paucialveolata* Grimsdale, 1952*, A. striata* Todd & Post, 1954*, Bigenerina* spp., *Bolivina* spp, *Borelis haueri* de Montfort, 1808*, B. merici* Sirel & Gunduz, 1981*, B. pygmaea* Hanzawa, 1930*, Brizalina* spp., *Bullalveolina* spp., *Carpenteria* spp., *Cibicides* spp., *Dendritina rangi* Orbigny, *emend.* Fornasini, 1904, *Discorbis* spp., *Elphidium* spp., *Eulepidina* sp*., E. dilatata* (Michelotti 1861), *Glomospira* spp., *Glomospirella* spp., *Gypsina* spp., *Haddonia* spp., *Halkyardia maxima* Cimmerman, 1969*, Halkyardia* spp., *Haplophragmium* spp., *Heterillina* spp., *Heterolepa* spp., *Heterostegina* spp., *Idalina* spp., *Lenticulina* spp., *Massilina* spp., *Miogypsinoides* spp., *Neoeponides* spp., *Neorotalia vienotti* Greig, 1935*, Nephrolepidina* spp., *Nodosaria* spp., *Nummoloculina* sp., *Operculina complanata* (Defrance), *Peneroplis evolutus* Henson, 1950*, P. thomasi* Henson, 1950*, Planorbulina* spp., *Praerhapidionina* sp*., Pseudolituonella reicheli* Marie, 1955*, Pyrgo* spp., *Quinqueloculina* spp., *Reussella* spp., *Risananeiza pustulosa* Boukhary, Kuss and Abdelraouf, 2008*, Schlumbergerina* spp., *Spirolina* sp., *Spiroloculina* spp*., Sphaerogypsina globulus* (Reuss), *Textularia* spp., *Triloculina* spp., *T. tricarinata* d' Orbigny, 1826*, T. trigonula* (Lamarck), *Uvigerina* spp., *Valvulina* sp.1, *Valvulina* spp.

APPENDIX 2

Comparison of foraminiferal contents of the Kharzan section with those of adjacent sections

Reference	Yazdi-Moghadam (2011)	Mohammadi et al. (2013)		Karavan et al. (2014)	Mohammadi et al. (2015)			Mohammadi and Ameri (2015)	Yazdi-Moghadam et al., (2018 a)	Basso et al. (2019)	Akbar-Baskalayeh et al. (2020)	This Study
Name of section	Baranduz section	Ghohroud section	Vidoja section	Bijgan section	Bujan section	Varkan section	Khurabad section	Abadeh area	Sonqor section	Uromieh section	Tajar-kuh section	Kharzan section
Thickness (m)	126	325	410	145.5	155	190	300	85	553	93	175	422
Coordinates (latitude; longitude)	37º20.59´N, 44º56.26´E	33º37´44"N, 51º24´24"E	33º51´31"N, 51º09´14"E	34°03'47"N, 50°46'16"E	29°26′04″N, 55°59′27″E	33°41′29N, 51°04′54″E	34°30′53″N, 50°56′58″E	31°31′26.77″N, 52°48′36.46″E	34º50´00˝N, 47º37´10.9˝E	37º20´35.4˝N, 44º56´15.6˝E	34°04'0.1"N, 51°05'45.3"E	33°24'36"N, 52°05' 57"E
Age	early–middle Rupelian	Rupelian–Chattian	Rupelian	Rupelian–Chattian	Rupelian–Chattian	Rupelian	Rupelian–Burdigalian	Rupelian-Chattian	early Rupelian	Rupelian	late Rupelian to early Chattian	Chattian
Genera/species												
Lepidocyclinids								*				
Nummulites sp.		*	*	*	*	*	*	*		*		
Nummulites vascus		*	*			*	*		*	*		
Nummulites sp. cf. *N. vascus*	*	*		*								
Nummulites fichteli		*	*	*	*	*			*	*		
Heterostegina sp.	*		*	*	*	*		*		*		*
Operculina sp.	*	*	*	*		*	*	*		*		
Amphistegina sp.		*	*	*	*	*	*	*				*
Peneroplis sp.		*	*					*		*		
Archaias sp.			*		*	*		*				
Textulariids		*	*	*	*	*	*	*	*			*
Miliolids		*	*	*	*	*	*	*	*	*		*
Rotaliids								*				
Neorotalia viennoti		*	*	*	*	*		*				*
Planorbulinids	*							*		*		*
Nummulites bormidiensis											*	
Nummulites kecskemetii											*	
Heterostegina assilinoides											*	
Nephrolepidina praemarginata											*	
Nephrolepidina praemarginata											*	
Eulepidina ex. interc. *formosoides* et *dilatata*											*	
Planolinderina sp.			*								*	
Nephrolepidina sp.		*	*	*	*	*	*					*
Nephrolepidina sp. cf. *N. marginata*			*									
Nephrolepidina tournoueri		*			*	*	*					
Eulepidina sp.		*	*	*	*	*	*					*
Eulepidina dilitata		*		*	*							*
Austrotrillina howchini		*	*	*	*	*						

Bigenerina sp.				*								*
Neorotalia sp.	*	*	*	*	*	*	*		*	*		
Lepidocyclina sp.		*	*	*	*	*	*					
Operculina complanata	*	*	*	*	*	*	*		*			*
Peneroplis sp. cf. *P. evolutus*				*								
Peneroplis thomasi	*	*		*		*						*
Sphaerogypsina sp.			*		*	*						
Sphaerogypsina globulus				*		*				*		*
Elphidium sp.		*	*	*		*	*					*
Discorbis sp.		*	*	*								*
Borelis pygmaea		*	*	*	*	*						*
Archaias kirkukensis					*							
Borelis sp.	*	*	*	*						*		*
Valvulinid		*	*	*					*			*
Globigerina angulisuturalis			*									
Globorotalia opima			*									
Peneroplis farsensis				*								
Penarchaias glynnjonesi	*								*	*		
Halkyardia maxima									*	*		*
Praerhapydionina delicata	*								*	*		
Praerhapydionina sp.												*
Haddonia sp.										*		*
Asterigerinoidea										*		
Victoriella sp.										*		
Dendritina rangi	*		*		*	*				*		*
Dendritina sp.		*	*									
Neorotalia lithothamnica	*											
Asterigerina sp.	*		*									
Planorbulina bronnimanni	*								*			
Victoriella conoidea	*											
Halkyardia minima	*											
Globigerina praebulloides	*											
Globigerina tripartita	*											
Paragloborotalia nana	*											
Chiloguembelina cubensis	*											
Subbotina yeguaensis	*											
Nummulites sp. cf. *N. fichteli*	*											
Spirolina sp.cf. *S. cylindracea*	*											
Bullaveolina sp.	*								*			
Globigerina sp.			*									
Austrotrillina sp.	*	*	*		*	*	*					
Asterigerina rotula									*			*
Discogypsina discus									*			
Gypsina mastelensis									*			
Stomatorbina concentrica									*			
Austrotrillina sp. aff. *A. paucialveolata*									*			
Haddonia heissigi									*			

Carpenteria sp.									*			
Eponides sp.									*			
Neoeponides sp.												*
Planulina sp.									*			
Lobatula sp.									*			
Stomatorbina concentrica									*			
Discogypsina discus									*			
Gypsina sp.												*
Risananeiza pustulosa												*
Peneroplis evolutus		*	*									*
Austrotrillina paucialveolata												*
Lenticulina sp.			*									*
Idalina sp.												*
Borelis haueri					*	*						*
Sorites sp.			*									
Austrotrillina asmariensis		*	*		*							*
Globigerinoides ciperoensis			*									
Globigerinoides sp. cf. *G. subquadratus*			*									
Nodosaria spp.												*
Miogypsinoides spp.												*
Austrotrillina striata			*									*
Bolivina spp.												*
Brizalina spp.												*
Halkyardia spp.												*
Pseudolituonella reichelli												*
Uvigerina spp.												*
Schlumbergerina sp.			*									*
Heterolepa spp.												*
Glomospira spp.												*
Haplophragmium sp.						*						*
Cibicides sp.						*						*
Reussella sp.												*
Borelis merici												*
Glomospirella spp.												*
Nummoloculina sp.												*
Spirolina sp.												*

APPENDIX 3

Facies identified in the Kharzan section

Facies no.	Facies type	Components	Depositional environment
Mf1	Marl or silty marl	Benthic foraminifera (miliolids) and ostracods	Restricted lagoon
Mf2	Silty mudstone	Limy mudstone matrix with scattered silt-sized detrital quartz grains	Restricted lagoon
Mf3	Imperforate foraminiferal wackestone-packstone	Porcellaneous foraminifera (miliolids, *Borelis, Dendritina, Austrotrillina, Peneroplis*) in a micritic matrix, coralline red algae, echinoderms, agglutinated foraminifera, ostracods, gastropods, and bivalves, sporadic quartz (10–15%)	Restricted lagoon
Mf4	Imperforate foraminiferal packstone-grainstone	Imperforate foraminifera (miliolids, peneroplids, and alveolinids), red algal fragments, gastropods, bivalves, echinoids, and foraminifera with agglutinated shells. peloids and detrital quartz grains may reach 10%	Lagoon
Mf5	Red algal-foraminiferal packstone-grainstone	Hyaline-walled foraminifera (*Amphistegina, Neorotalia*, *Asterigerina*, and swollen and small Lepidocyclinidae, *Elphidium*), imperforate foraminifera (miliolids), coralline red algae, bryozoans, coral, echinoderms, ostracods, gastropods, bivalves, and agglutinated foraminifera.	Open marine lagoon
Mf6	Coral boundstone	About 90% colonial corals, foraminifera (miliolids and *Borelis*)	Patch reefs, in lagoon settings
Mf7	Coralline red algal-coral packstone-rudstone	Red algae and corals, Hyaline-walled benthic foraminifera (*Amphistegina,* and *Lepidocyclina*), echinoderm fragments, bivalves, and bryozoans larger than 2 mm in size	The lower part of the reef belt and the upper part of the slope
Mf8	Perforate foraminiferal wackestone-packstone	Perforated foraminifera (*Eulepidina*), *Heterostegina, Operculina*, *Neorotalia*, *Amphistegina*), bryozoans, echinoderms, ostracods, gastropods, bivalves, coralline red algae	The lower part of a slope